

This is an Open Access document downloaded from ORCA, Cardiff University's institutional repository:<https://orca.cardiff.ac.uk/id/eprint/182072/>

This is the author's version of a work that was submitted to / accepted for publication.

Citation for final published version:

Gao, Zhenghui, Cleall, Peter J. , Sapsford, Devin J. , Steer, Julian and Harbottle, Michael J. 2025. A nature-based approach to enhance the potential application of forest residues in anaerobic digestion. *Journal of Environmental Management* 395 , 127763. 10.1016/j.jenvman.2025.127763

Publishers page: <https://doi.org/10.1016/j.jenvman.2025.127763>

Please note:

Changes made as a result of publishing processes such as copy-editing, formatting and page numbers may not be reflected in this version. For the definitive version of this publication, please refer to the published source. You are advised to consult the publisher's version if you wish to cite this paper.

This version is being made available in accordance with publisher policies. See <http://orca.cf.ac.uk/policies.html> for usage policies. Copyright and moral rights for publications made available in ORCA are retained by the copyright holders.



1 **A nature-based approach to enhance the**  
2 **potential application of forest residues in**  
3 **anaerobic digestion**

4 **Zhenghui Gao**<sup>a,b\*</sup>, **Peter J. Cleall**<sup>b</sup>, **Devin J. Sapsford**<sup>b</sup>, **Julian Steer**<sup>b</sup>, **Michael J. Harbottle**<sup>b</sup>

5 <sup>a</sup> Key Lab of Urban Environment and Health, Institute of Urban Environment, Chinese Academy of Sciences,  
6 Xiamen 361021, China

7 <sup>b</sup> School of Engineering, Cardiff University, Cardiff CF24 3AA, UK

8

9 **Author Information**

10 **Corresponding Author**

11 **Zhenghui Gao** - Key Lab of Urban Environment and Health, Institute of Urban Environment,  
12 Chinese Academy of Sciences, Xiamen 361021, China; School of Engineering, Cardiff  
13 University, Cardiff CF24 3AA, UK; <https://orcid.org/0000-0002-0431-0626>; Email:  
14 [zhgao@iue.ac.cn](mailto:zhgao@iue.ac.cn)

15 **Authors**

16 **Peter J. Cleall** - School of Engineering, Cardiff University, Cardiff CF24 3AA, UK;  
17 <https://orcid.org/0000-0002-4005-5319>

18 **Devin J. Sapsford** - School of Engineering, Cardiff University, Cardiff CF24 3AA, UK;  
19 <https://orcid.org/0000-0002-6763-7909>

---

\* Corresponding author: [zhgao@iue.ac.cn](mailto:zhgao@iue.ac.cn)

20 **Julian Steer** - School of Engineering, Cardiff University, Cardiff CF24 3AA, UK;

21 <https://orcid.org/0000-0002-3003-4768>

22 **Michael J. Harbottle** - School of Engineering, Cardiff University, Cardiff CF24 3AA, UK;

23 <https://orcid.org/0000-0002-6443-5340>

# A nature-based approach to enhance the potential application of forest residues in anaerobic digestion

**Abstract:** Forest residues and other woody wastes are abundant and require management. Anaerobic digestion (AD) is a potential disposal option for such waste, but the absence of cost-effective pretreatment technologies hinders their utilization in AD. This paper presents a nature-based approach for improving AD performance of forest residues, relying on the lignocellulose degradation processes inherent in the forest ecosystem. Wood samples at five decay classes (numbered 1-5 with increasing decay) were collected for series of experiments. Physicochemical analysis showed that higher decay class samples presented a series of characteristics favourable to AD. Wood samples from decay class 1 had the lowest methane yield, while decay class 3 had the highest, with a notable 160% increase compared to decay class 1. The outcomes identify the stage of highest methane production from forest residues, allowing for strategic collection to improve the economic viability of using forest residues as feedstock for AD applications.

**Keywords:** Forest residues; Woody waste; Anaerobic digestion; Methane production; Pretreatment technology; Forest soil ecosystem

## Nomenclature

AD: anaerobic digestion; DC: decay class; VS: volatile solids; SEC: specific energy consumption; MWD: mean weight diameter; FD: fractal dimension; TS: total solids; TOC: total organic carbon; WEOC: water extractable organic carbon; CrI: cellulose crystallinity index; ORP: oxidation reduction potential; TMP: theoretical methane production; BD: anaerobic biodegradability; EMP: experimental methane production; PMP: predicted methane production.

## 1 Introduction

The anaerobic digestion (AD) of renewable biomass, including woody biomass, is emerging as a sustainable energy source due to its availability, low cost, and minimal environmental impact (Gao et al., 2025; Manikandan et al., 2023). Recent studies highlight that pretreatment techniques significantly enhance methane production from woody biomass, underscoring its potential as a AD feedstock (Gao et al., 2024a). A variety of pretreatment approaches have been developed to breakdown the recalcitrant structure of woody biomass, including biological, chemical, and physical processes (Gao et al., 2022; Hashemi et al., 2022). While physical methods require large energy inputs and high equipment cost for the specific conditions (Atelge et al., 2020; Gao et al., 2024b), and chemical methods risk environmental contamination (Dai et al., 2018; Tian et al., 2016), biological methods show potential despite challenges in isolating effective microorganisms and the lengthy, labor-intensive process (Alexandropoulou et al., 2017; Ali et al., 2017). In view of this, it is important to consider and develop alternative technologies for the pretreatment of woody biomass to boost methane production in a more sustainable way.

1 43 In forest ecosystems, dead trees play a crucial ecological role by decomposing and  
2  
3  
4 44 releasing stored nutrients (Seibold et al., 2021). The decomposition process, involving fungi,  
5  
6 45 bacteria, and arthropods, spans several years and creates a complex community (Tarasov et  
7  
8  
9 46 al., 2018; Yoon et al., 2023). Due to the complexity of the natural wood degradation process  
10  
11  
12 47 in forest ecosystems, it is difficult to simulate and apply this system as a pretreatment method  
13  
14  
15 48 for woody biomass under experimental conditions. Notably, large quantities of forest  
16  
17  
18 49 residues are generated during timber harvesting and from forest maintenance treatments such  
19  
20  
21 50 as cleaning and thinning (Pergola et al., 2022). It is estimated that there are approximately  
22  
23  
24 51 230,000 hectares of plantation forests in Queensland, with up to 600,000 tons of forest  
25  
26  
27 52 residues generated by logging annually (Garvie et al., 2021). Kurvits et al. (2020)  
28  
29  
30 53 investigated the quantity of logging residues at four forest sites in Southeast Estonia from  
31  
32  
33 54 2013 to 2014 and found that forest residues reached up to a dry weight of 29 tons per hectare.  
34  
35  
36 55 Unless harvested for application, the fate of these forest residues is to be degraded into humus  
37  
38  
39 56 as part of the forest soil. During this degradation process, the texture of the wood will  
40  
41  
42 57 gradually become soft, as the rigid and recalcitrant lignocellulosic structure is slowly  
43  
44  
45 58 destroyed, with the wood finally being completely decomposed to release all the nutrients  
46  
47  
48 59 (Petritan et al., 2023; Shorohova et al., 2021).

49 60 An interesting aspect of this natural degradation process is that it tends to predispose  
50  
51  
52 61 wood waste for AD applications due to the increased accessibility and biodegradability of  
53  
54  
55 62 the lignocellulosic structure. In addition, the softened texture of the material allows them to  
56  
57  
58 63 be shredded more easily, which can also save the energy required to pre-process the material  
59  
60  
61 64 prior to AD. We hypothesize that exposing woody wastes to forest ecosystems for a period

1 65 of time is sufficient to enhance its digestibility as part of a pretreatment process prior to AD.  
2  
3  
4 66 In addition, the collection and valorisation of such residues can help to mitigate forest  
5  
6 67 management costs, reducing fire risk and additional emissions from degradation (Lee and  
7  
8  
9 68 Han, 2017; Molenda et al., 2021; Nicholls et al., 2018). The objectives of this study were to  
10  
11  
12 69 determine the differences in physicochemical composition and the methane production  
13  
14  
15 70 potential between wood samples at different stages of decay from forest environments.  
16  
17  
18 71 Identifying the decay stage at which the wood waste can have the highest methane production  
19  
20  
21 72 allows for strategic collection of this material, enhancing the economic viability of using  
22  
23  
24 73 wood waste as a raw material in AD applications.

## 27 74 **2 Materials and methods**

### 30 75 **2.1 Experimental materials**

33 76 The wood samples were collected from two sites, with Site 1 being an unmanaged  
34  
35  
36 77 seminatural forest in Cardiff, UK (51°31'4"N, 3°14'46"W) and Site 2 being a large managed  
37  
38  
39 78 forest in Cardiff, UK (51°32'25"N, 3°14'58"W). At each site, at least 15 dead fallen logs were  
40  
41  
42 79 sampled, each of which was allocated to a particular *decay class* (DC), determined based on  
43  
44  
45 80 visual and mechanical inspections (Table S1), with DC1 showing minimal signs of decay and  
46  
47  
48 81 DC5 showing highly advanced levels of decay (Tatti et al., 2018). Considering the external  
49  
50  
51 82 appearance and the species of the surrounding trees, the wood samples from Site 1 were  
52  
53  
54 83 probably hardwood silver birch (*Betula pendula*), expressed here as Birch. The sampling  
55  
56  
57 84 location at Site 2 consists primarily of European ash (*Fraxinus excelsior*), expressed in this  
58  
59  
60 85 paper as Ash, confirmed from site records and by examining the surrounding tree morphology.  
61  
62  
63  
64  
65

1 86 Wood samples were dried and then shredded using a Fritsch 55743 rotary knife mill with a 2  
2  
3  
4 87 mm screen and finally stored at 4 °C until further analysis.  
5  
6

## 7 88 2.2 Experimental procedure

8  
9  
10 89 The AD experimental apparatus, consisting of multiple 1L bioreactors in a temperature-  
11  
12  
13 90 controlled water bath with gas collection facility, was supplied by Anaero Technology UK,  
14  
15  
16 91 described in more detail by Muaaz-Us-Salam et al. (2020). Sewage sludge digestate from an  
17  
18  
19 92 AD reactor was used as an anaerobic inoculum. Prior to AD testing, the sludge was incubated  
20  
21  
22 93 at 35 °C for 3 days and shaken manually twice a day to ensure homogenization. For every  
23  
24  
25 94 experiment, fresh sludge was sampled from the same AD reactor. Each bioreactor was filled  
26  
27  
28 95 with 700 mL of inoculum with a headspace volume of 300 mL. Then a certain mass of wood  
29  
30  
31 96 samples at different DC was added, the blank group did not have any wood sample added  
32  
33  
34 97 (only 700 mL inoculum). The weight of wood samples in each reactor was calculated to  
35  
36  
37 98 ensure the ratio of decaying wood samples to inoculum was 1:4 based on volatile solids (VS)  
38  
39  
40 99 levels. All bioreactors were incubated at 35 °C for 35 days with continuous stirring at 45 rpm.  
41  
42 100 Liquid samples (5 mL) were taken during the AD process using sterile pipettes and  
43  
44  
45 101 transferred to 15 mL sterile containers for the measurement of some parameters during the  
46  
47  
48 102 AD process. Biogas produced from each reactor was collected during the experiment in 5 L  
49  
50  
51 103 Tedlar gas bags and analyzed for methane content (see section 2.3.4). The AD experiments  
52  
53  
54 104 were performed in triplicate for each wood sample and in duplicate for the blank group (only  
55  
56  
57 105 inoculum).  
58

## 59 106 2.3 Analytical methods

### 2.3.1 Specific energy consumption for grinding

The effect of DC on specific energy consumption (SEC) during shredding (comminution) was determined. A Fritsch 55743 rotary knife mill was used, equipped with a 2 mm screen and a 2100 W motor. For all samples, a pre-weighed 50 grams wood block (dry matter) was placed in the rotary knife mill for 60 seconds, and then the wood collected in the tray was weighed. The SEC was calculated according to Equation (1) as presented in previous literature (Miao et al., 2011; Moiceanu et al., 2019).

$$\text{SEC} = \frac{P \times T}{m} \quad (1)$$

where SEC is total specific energy consumption for grinding a unit of dry matter (MJ/kg of dry matter);  $P$  is the power of the milling machine while grinding wood samples;  $T$  is the total time of grinding operations;  $m$  is dry matter mass (kg) of wood samples collected in the tray.

### 2.3.2 Analysis of particle size distribution

Particle size distribution was measured using sieving methods. Specifically, wood samples were put into a Fritsch 55743 rotary knife mill equipped with a 2 mm screen and operated for 1 min. The collected sample was passed through a tower of differently sized sieves. The sieve stack contained stainless steel sieves (diameter 200 mm) with mesh sizes of 2000, 1000, 500, 250, 125, and 75  $\mu\text{m}$ . The sieving steps were performed on a vibratory shaker (Matest A060-01) for 30 min to ensure adequate separation of the samples. Samples were finally sieved into seven fractions (<75, 75–125, 125–250, 250–500, 500–1000, 1000–2000, and >2000  $\mu\text{m}$ ), and the proportion of samples in each particle size class was calculated based on the weight.

1 128 The mean weight diameter (MWD) and fractal dimension (FD) can be applied to further  
2  
3  
4 129 characterize the particle size of the sample (Rabot et al., 2018; Zhang et al., 2021). MWD is  
5  
6 130 the sum of the weighted mean diameters of all size classes, whilst FD is a comprehensive  
7  
8  
9 131 indicator of sample composition and textural homogeneity. The MWD of dry-sieved samples  
10  
11  
12 132 was calculated using Equation (2):

$$\text{MWD} = \sum_{i=1}^n \frac{r_i + r_{i+1}}{2} \times m_i \quad (2)$$

13 133 where  $r_i$  is the aperture of the  $i$ th sieve,  $m_i$  is the proportion of sample weight remaining on  
14  
15  
16  
17  
18  
19  
20  
21  
22 134 the  $i$ th sieve, and  $n$  is the number of sieves. The FD was calculated using Equation (3):

$$\frac{M(r < R_i)}{M_r} = \left(\frac{R_i}{R_{max}}\right)^{3-FD} \quad (3)$$

23  
24  
25  
26  
27  
28 135 where  $M(r < R_i)$  is the cumulative sample mass with a radius smaller than  $R_i$ ,  $M_r$  is the total  
29  
30  
31  
32 136 sample mass with a radius smaller than  $R_{max}$ ,  $R_i$  is the radius of each dimensional fraction,  
33  
34 137  $R_{max}$  is the maximum radius, and FD is the fractal dimension of the sample.

### 35 36 37 138 2.3.3 Physicochemical features of solid samples

38  
39  
40 139 Total solids (TS) and VS of the wood samples were measured following the Standard  
41  
42  
43 140 Methods 2540 protocol (Rice et al., 2017). The ultimate analysis (carbon, hydrogen, nitrogen,  
44  
45  
46 141 and oxygen content) was measured using an elemental analyzer (Flash Smart, Thermo Fisher  
47  
48  
49 142 Scientific Co., USA). Cellulose, hemicellulose, and lignin contents were determined by  
50  
51  
52 143 thermogravimetric analysis (Díez et al., 2020; Rego et al., 2019), and the detailed approach  
53  
54 144 is shown in the Supporting Information (Text S2). The total organic carbon (TOC) of wood  
55  
56  
57 145 samples were measured with a TOC-VCPH (Shimadzu, Kyoto, Japan) following the  
58  
59  
60 146 manufacturer's instructions. The analysis of water extractable organic carbon (WEOC) was

1 147 modified from Mo et al., (2022). Specifically, a total of 5 g of shredded wood was added to  
2  
3  
4 148 30 mL of Milli-Q water and shaken at 200 rpm for 2 h at room temperature. The supernatant  
5  
6 149 was subsequently filtered through sterile 0.45  $\mu\text{m}$  filters and stored in the dark at 4  $^{\circ}\text{C}$  prior  
7  
8  
9 150 to further analyses. Finally, the WEOC concentrations were measured by a TOC-VCPH  
10  
11  
12 151 (Shimadzu, Kyoto, Japan) following the manufacturer's instructions.  
13  
14

15 152 The crystallinities of all decaying wood samples were measured using a X'Pert<sup>3</sup> MRD  
16  
17  
18 153 XL Materials Research X-ray Diffraction System (Malvern Panalytical, Malvern, UK)  
19  
20  
21 154 equipped with with CuK $\alpha$  radiation. Scans were obtained from  $2\theta = 10\text{--}40^{\circ}$  with step size of  
22  
23  
24 155 0.02 at 0.6 s per step. The cellulose crystallinity index (CrI) of the samples can be calculated  
25  
26  
27 156 according to Equation (4):

$$\text{CrI} = \frac{I_{002} - I_{am}}{I_{002}} \times 100 \quad (4)$$

28  
29  
30  
31  
32  
33 157 where  $I_{002}$  is intensity of diffraction from 002 plane at  $2\theta = 22^{\circ}$  and  $I_{am}$  is the intensity of  
34  
35  
36 158 background measured at  $2\theta = 18^{\circ}$  (Kumar et al., 2019; Liu et al., 2015).  
37  
38

### 39 159 2.3.4 Physicochemical features of liquid and gas samples 40 41

42 160 TS and VS of the inoculum were measured following the standard methods (Rice et al.,  
43  
44  
45 161 2017). The inoculum was dried and subjected to ultimate analysis with an elemental analyzer  
46  
47  
48 162 (Flash Smart, Thermo Fisher Scientific Co., USA). The pH and oxidation reduction potential  
49  
50  
51 163 (ORP) of inoculum and liquids samples collected during AD experiments were measured by  
52  
53  
54 164 a freshly calibrated pH probe (Mettler-Toledo, Switzerland) and a freshly calibrated ORP  
55  
56  
57 165 probe with an Ag/AgCl electrode (Mettler-Toledo, Switzerland). All 5 mL liquid samples  
58  
59 166 obtained during AD experiments were filtered through sterile 0.45  $\mu\text{m}$  filters. Subsequently,  
60  
61  
62  
63  
64  
65

1 167 a 2 mL filtered sample was added to 18 mL Milli-Q water (10 times dilution) and mixed  
2  
3  
4 168 thoroughly for TOC measurement.  
5

6 169 The biogas production in each bioreactor was determined by gas flow meters  
7  
8  
9 170 incorporated within the AD apparatus combined with data logging equipment, and the  
10  
11  
12 171 methane content of the biogas was determined using a portable biogas analyzer (RASI 700  
13  
14  
15 172 BIO, Eurotron Instruments UK ltd, Germany). The instrument was calibrated using a series  
16  
17  
18 173 of standard gases with concentration gradients (labeled methane concentration) prior to  
19  
20  
21 174 testing the methane content in the samples.  
22

### 23 175 2.3.5 Calculation and prediction of methane production

26 176 The theoretical methane production (TMP) of wood samples was calculated from the  
27  
28  
29 177 elemental composition (expressed in molar fractions) using the Buswell formulae (Lübken et  
30  
31  
32 178 al., 2010), Equations (5) and (6):  
33

$$34 \quad C_n H_a O_b N_c + \left( n - \frac{a}{4} - \frac{b}{2} + \frac{3c}{4} \right) H_2O$$
$$35 \quad \rightarrow \left( \frac{n}{2} + \frac{a}{8} - \frac{b}{4} - \frac{3c}{8} \right) CH_4 + \left( \frac{n}{2} - \frac{a}{8} + \frac{b}{4} + \frac{3c}{8} \right) CO_2 + cNH_3$$

36  
37  
38  
39  
40  
41

$$42 \quad TMP = 22.4 \times \left( \frac{n}{2} + \frac{a}{8} - \frac{b}{4} - \frac{3c}{8} \right) / (12n + a + 16b + 14c)$$

43  
44  
45

46 179 The anaerobic biodegradability (BD) of wood samples was calculated according to  
47  
48  
49 180 Equation (7):  
50

$$51 \quad BD (\%) = \text{Experimental methane production (EMP)} / TMP \times 100$$

52  
53  
54

55 181 The experimental biogas production was fitted using a modified Gompertz kinetic model,  
56  
57 182 which is one of the most commonly employed models in the literature for fitting biogas  
58  
59  
60 183 production (Isha et al., 2021). The final biogas production was calculated based on the best-  
61  
62

1 184 fit Gompertz model and then multiplied by the methane content to obtain the predicted  
2  
3  
4 185 methane production (PMP). The kinetic model is shown in Equation (8):

$$M = P_b \times \exp \left\{ -\exp \left[ \frac{R_m \times e}{P_b} (\lambda - t) + 1 \right] \right\} \quad (8)$$

5  
6  
7  
8  
9  
10 186 where  $M$  is the biogas production (mL/g of VS) relative to the time  $t$  (d);  $P_b$  is the maximum  
11  
12  
13 187 biogas potential of the substrate (mL/g of VS);  $R_m$  is the maximum biogas production rate  
14  
15  
16 188 (mL/g of VS.d),  $\lambda$  is the lag phase time taken for biogas production (1/d),  $e$  is Euler's number  
17  
18  
19 189 which is taken here as 2.7183.

20  
21  
22 190 Furthermore, there was no well-developed model available to predict the methane  
23  
24  
25 191 production from AD of wood waste. Our previous study generated a machine learning model  
26  
27  
28 192 with good predictive performance, which was applied in this study to predict methane  
29  
30  
31 193 production from all decayed wood samples (Gao et al., 2024a). In the previous publication,  
32  
33  
34 194 1179 groups of datasets were collected for the machine learning analysis, which included  
35  
36  
37 195 nine input variables, namely wood types, inoculum types, volume (mL), temperature (°C),  
38  
39  
40 196 particle size (mm), ratio of inoculum to substrate (based on VS), cellulose content (%),  
41  
42  
43 197 hemicellulose content (%), lignin content (%), and digestion time (d), where wood types and  
44  
45  
46 198 inoculum types were represented as categorical objects. The random forest machine learning  
47  
48  
49 199 method was found to have the highest prediction accuracy and was used in this study.

## 50 51 200 2.4 Statistical analysis

52  
53  
54 201 In this paper, statistical analyses were done using Origin 2021. All values are presented  
55  
56  
57 202 as the mean  $\pm$  s.d., unless otherwise specified. Statistical significance was assessed using the  
58  
59  
60 203 two-tailed Student's t-test or One-way ANOVA test with significance at a  $p$  value of 0.05.

1 204 Moreover, The Pearson correlation coefficients ( $r$ ) between the variables were also calculated.

2  
3 205 The strength of the correlation was described by the absolute value of  $r$  (0.00–0.19 very weak;  
4  
5  
6 206 0.20–0.39 weak; 0.40–0.59 moderate; 0.60–0.79 strong; 0.80–1.0 very strong).

## 9 207 **3 Results and discussion**

### 12 208 **3.1 Energy consumption and particle size analysis**

16 209 Generally, mechanical pretreatment is considered as the most important and promising  
17  
18 210 preliminary step for handling and converting biomass into bioenergy before proceeding to  
19  
20  
21  
22 211 the next process (Kamarludin et al., 2014). Without a sufficiently small particle size or large  
23  
24  
25 212 relative surface area, the organic matter in the substrate cannot be utilized by microorganisms  
26  
27  
28 213 to produce biogas during AD. For example, 2 cm wood cubes in digested sewage sludge  
29  
30  
31 214 produced approximately the same amount of biogas as blanks with only sludge (Gao et al.,  
32  
33 215 2023; Muaaz-Us-Salam et al., 2020). As shown in Fig. 1, the SEC gradually decreased as DC  
34  
35  
36 216 increased. Fig. 1a shows that the SEC of Birch decreased from 10.56 to 2.92 MJ/kg of dry  
37  
38  
39 217 matter for DC1 to DC5, while Ash correspondingly dropped from 9.44 to 2.60 MJ/kg of dry  
40  
41  
42 218 matter (Fig. 1b). In addition, the decrease rate of SEC for both wood samples gradually  
43  
44  
45 219 became slower with increased DC, showing no statistical difference between wood samples  
46  
47  
48 220 from DC3 to DC5. These results imply that the higher the DC, the more energy can be saved  
49  
50  
51 221 in reducing the particle size of these wood samples for utilization in AD. It is worth noting  
52  
53  
54 222 that the criteria for these DC include their hardness, with DC5 being extremely soft due to its  
55  
56 223 woody structure has been essentially destroyed (Tatti et al., 2018). During the sampling, it

1 224 was found that DC4 and DC5 can be broken even with slight force by hand. Therefore, wood  
2  
3  
4 225 samples with high DC may not require physical pre-processing.  
5

6 226 Reducing the particle size of substrates is a competitive option for increasing methane  
7  
8  
9 227 production from AD as it releases more organic matter and cell compounds, and directly  
10  
11  
12 228 increases the microbially accessible surface area, thus improving biodegradability (Dai et al.,  
13  
14  
15 229 2019). After grinding the samples, we analyzed their particle size distribution (Table 1). The  
16  
17  
18 230 samples of DC1 and DC2 had the highest proportion in the 1–2 mm particle size class, and  
19  
20  
21 231 the proportion decreased as the particle size class increased. The proportion of the fine  
22  
23  
24 232 particle size class gradually increased from DC1 to DC5, with the proportion of 0.5–1 mm  
25  
26  
27 233 particle size class being the largest in DC4 and DC5. In addition, the MWD analysis also  
28  
29  
30 234 showed the particle size of wood samples reduced gradually from DC1 to DC5. Specifically,  
31  
32  
33 235 the MWD of Birch decreased from 0.93 to 0.57 mm for DC1 to DC5, while Ash  
34  
35  
36 236 correspondingly dropped from 1.10 to 0.78 mm (Table 1). Reduced particle size can  
37  
38  
39 237 significantly facilitate hydrolysis and acidification processes, resulting in increased volatile  
40  
41  
42 238 fatty acid content and VS degradation (Luo et al., 2021). Liu et al. (2017) reported the effects  
43  
44  
45 239 of particle size of two forest residues on methane production through AD batch experiments,  
46  
47  
48 240 and the results showed that methane yield improved when the substrate particle size was  
49  
50  
51 241 reduced from 4 mm to 1 mm. A similar pattern has been demonstrated in other lignocellulosic  
52  
53  
54 242 wastes, such as rice straw, where methane production improved with a decrease in substrate  
55  
56  
57 243 particle size (Dai et al., 2019; Ji et al., 2022).

58 244 Fractal theory has been applied to quantitatively assess the basic morphology of the  
59  
60  
61 245 substrate, which is a potential indicator reflecting the AD efficiency (Wang et al., 2016). In  
62  
63  
64  
65

1 246 this study, the FD of different DC samples were statistically different ( $p<0.05$ ) after grinding  
2  
3  
4 247 under the same conditions. As shown in Table 1, the FD average of both wood samples at  
5  
6 248 DC1 was significantly lower than DC5 ( $p<0.05$ ), while there were no significant differences  
7  
8  
9 249 in FD values between DC3, DC4 and DC5 ( $p>0.05$ ). The increase in FD can enhance the  
10  
11  
12 250 particle translational velocities in the horizontal direction while decreasing the rotational  
13  
14  
15 251 velocity, and the amount of particles participated in horizontal dispersion increased due to  
16  
17  
18 252 the reduction in the intensity of the contact shear particle behavior, which effectively  
19  
20  
21 253 promoted particle diffusion (Lai et al., 2021). Therefore, the DC5 samples may have  
22  
23  
24 254 enhanced mobility in the AD system compared to the DC1 samples, which facilitates its full  
25  
26  
27 255 utilization by microbes. Moreover, the wood samples after DC3 showed no significant  
28  
29  
30 256 difference, suggesting that this class (DC3) may achieve optimal conditions for sample  
31  
32 257 crushing.

### 36 258 3.2 Physicochemical features analysis of decaying wood samples

39 259 The possibility of using these wood samples as a suitable substrate for AD was primarily  
40  
41  
42 260 verified through various tests, prior to conducting the biomethane potential experiments. As  
43  
44  
45 261 shown in Table 2, TS content decreased with DC, while the VS content did not change much.  
46  
47  
48 262 Samples with a high DC have a looser texture, which allows them to easily retain more water.  
49  
50  
51 263 Compared to Ash, in general Birch had a smaller TS content and a much larger drop from  
52  
53  
54 264 DC1 (59.47%) to DC5 (18.39%). For lignocellulosic biomass, the nitrogen content is a key  
55  
56  
57 265 factor limiting their AD performance (Song et al., 2024). A low level of nitrogen can lead to  
58  
59  
60 266 nitrogen limitation, which prevents the microorganisms from fully utilizing the carbon source,

1 267 thus reducing the production of methane (Piątek et al., 2016). The total carbon in all five DC  
2  
3  
4 268 were nearly the same, but the nitrogen content was higher in the high DC samples. Therefore,  
5  
6 269 the carbon to nitrogen ratio of DC5 was much lower than that of DC1. It has been reported  
7  
8  
9 270 that the optimal carbon to nitrogen ratio for maximal methane production is between 20 and  
10  
11  
12 271 30 (Kumar et al., 2021). Although the carbon to nitrogen ratio of DC5 samples was also  
13  
14  
15 272 higher than the optimal value, it is easier to achieve the superior system by mixing them with  
16  
17  
18 273 sludge (low carbon to nitrogen ratio). During AD, TOC can be biodegraded in hydrolysis,  
19  
20  
21 274 acidification and methanation steps to produce biogas (Provenzano et al., 2014). Furthermore,  
22  
23  
24 275 WEOC is a critical contributor in these processes, as microbial metabolism occurs in the  
25  
26  
27 276 water-soluble phase (Xing et al., 2012). Therefore, the significantly higher TOC (Fig. 2a and  
28  
29  
30 277 2b) and WEOC (Fig. 2c and 2d) in high DC samples indicate a better potential for methane  
31  
32  
33 278 production from AD. It is noteworthy that the WEOC did not consistently increase with decay  
34  
35  
36 279 level, showing a tendency of first increasing and then decreasing. The DC3 samples of Birch  
37  
38  
39 280 had the highest WEOC (Fig. 2c), and the DC4 samples of Ash had the highest WEOC (Fig.  
40  
41  
42 281 2d). This might be due to the release of organic matter from the forest residues in the presence  
43  
44  
45 282 of insects and microorganisms, leading to an increase in WEOC content at the beginning of  
46  
47  
48 283 decay process. When it reaches the final stages of decomposition, there is no more organic  
49  
50  
51 284 matter to be released, and the previously released organic matter is utilized by other  
52  
53  
54 285 organisms or enters the soil, leading to a decrease in the WEOC content.

55 286 The lignocellulose composition is an important factor that affects the AD performance  
56  
57  
58 287 of forest residues. Fig. S1 and S2 show the thermogravimetric experimental data and  
59  
60  
61 288 derivative thermogravimetric curves fitting results using the Gaussian model, and the

1 289 calculated lignocellulose composition of all wood samples are provided in Table 2. In both  
2  
3  
4 290 types of wood samples, the cellulose content decreased with DC, in contrast with a gradually  
5  
6 291 increased lignin content. The hemicellulose content did not vary much among the five DC  
7  
8  
9 292 samples, and two types of wood samples showed different tendencies. With an increase in  
10  
11  
12 293 DC, Birch presented an overall decrease, while Ash first decreased and then increased. The  
13  
14  
15 294 significantly increased lignin content of higher DC may be due to the reduction of other  
16  
17  
18 295 components such as cellulose, indicating that the forest soil system was not effective in  
19  
20  
21 296 removing lignin of forest residues, and it became proportionally more significant as a  
22  
23  
24 297 component as decay occurred. However, the decay has permitted biological access to, and  
25  
26  
27 298 degradation of, cellulose and hemicellulose, suggesting that a certain amount of decay and  
28  
29  
30 299 breakdown may be advantageous as a pretreatment method for AD. Similar effects have been  
31  
32  
33 300 observed in other studies, such as the application of chemicals (Mohsenzadeh et al., 2012;  
34  
35 301 Salehian et al., 2013), hydrothermal (Karami et al., 2022) and steam explosion (Eom et al.,  
36  
37  
38 302 2019; Mulat et al., 2018) leading to a reduction in the cellulose content and an increase in the  
39  
40  
41 303 lignin content of wood waste.

42  
43  
44 304 Due to the presence of crystalline cellulose in biomass samples, the  $2\theta$  value of X-ray  
45  
46  
47 305 diffraction shows a sharp peak between  $18^\circ$  and  $22^\circ$  (Awoyale and Lokhat, 2021). Cellulose  
48  
49  
50 306 crystallinity reflects the proportion of cellulose crystalline regions, and the CrI of the  
51  
52  
53 307 substrate determines its biodegradability during AD. The CrI of Birch DC1 samples was  
54  
55 308 35.43%, close to the value of raw pine wood; and the CrI of Ash DC1 samples (41.61%) was  
56  
57  
58 309 close to that of untreated acacias (Darmawan et al., 2016). It indicated that the degradation  
59  
60  
61 310 of DC1 samples was quite small, and its CR nearly approached that of fresh wood. The CrI

1 311 of DC5 samples was much lower than that of DC1 samples, with a value of 16.47% in Birch  
2  
3  
4 312 and 26.43% in Ash (Fig. 3). As mentioned above, this may be due to the different composition  
5  
6 313 in different DC samples. The content of soluble matter and amorphous cellulose in  
7  
8  
9 314 lignocellulosic biomass is higher than that of crystalline cellulose, which can result in a lower  
10  
11  
12 315 CrI (D' Silva et al., 2022). The hydrolysis of amorphous cellulose by cellulase was found to  
13  
14  
15 316 be about 30 times faster than that of crystalline cellulose (Zhu et al., 2011). The low CrI value  
16  
17  
18 317 in DC5 samples meant that their cellulose crystalline region was destroyed, leaving more  
19  
20  
21 318 cellulose (amorphous cellulose) available for microbial hydrolysis. Moreover, it was found  
22  
23  
24 319 that corn straw pretreatment with hydrogen-nanobubble water (He et al., 2022) or a pure  
25  
26  
27 320 bacteria system (Xu et al., 2018) also reduced the CrI of substrate and enhanced the methane  
28  
29  
30 321 production from AD of corn straw. Therefore, the forest soil system could degrade the  
31  
32  
33 322 cellulose crystallinity, allowing the forest residues to decompose more easily by AD.

### 34 35 36 323 3.3 Effect of five decay classes on anaerobic digestion performance

37  
38  
39 324 The patterns of daily biogas yield were shown in Fig. 4a and 4b. As higher DC samples  
40  
41  
42 325 had lower MWD (Table 1), resulting in a larger surface area, they would be more susceptible  
43  
44  
45 326 to hydrolysis and acidification compared to DC1 samples, producing more feedstock for  
46  
47  
48 327 methanogen utilization. To further explore the effects of particle size on biogas production,  
49  
50  
51 328 the Birch DC1 and DC3 samples with same particle size were selected for a separate AD  
52  
53  
54 329 experiment. Although the biogas yield of Birch DC3 samples was still considerably higher  
55  
56  
57 330 than that of DC1 samples, the gap between these samples at the same particle size was smaller  
58  
59  
60 331 than the previous (Fig. S3). It was also noted that all DC samples showed high daily biogas  
61  
62  
63  
64  
65

1 332 yield in the initial few days. During the early stages of AD, the feedstock is mainly  
2  
3  
4 333 hydrolyzed and acidified, and the primary contributors to the biogas are WEOC from the  
5  
6 334 wood samples and the residual organic matter in the sludge.  
7  
8

9 335 As shown in Fig. 4c and 4d, the net cumulative biogas yield varied significantly among  
10  
11  
12 336 different DC samples. These curves showed a rapid increase in biogas within the first 10 days,  
13  
14  
15 337 reaching about 50% of the total output. The final biogas yield increased from DC1 to DC3  
16  
17  
18 338 (Birch) and DC3/4 (Ash) before decreasing at higher DC. For Birch, the biogas yield of DC3  
19  
20  
21 339 samples was 3.52 times higher than that of DC1 samples, but this value narrowed down to  
22  
23  
24 340 2.14 at the same particle size (Fig. S3). This result suggested that decayed wood, besides  
25  
26  
27 341 increasing biogas production by being more prone to small particle sizes, had  
28  
29  
30 342 physicochemical properties that were more favorable for microbial utilization in AD system.  
31  
32 343 Fig. S4 illustrates the effect of DC on pH, ORP and TOC during AD. The initial phase of AD,  
33  
34  
35 344 which mainly involves the process of substrate hydrolysis and acidification, leads to a  
36  
37  
38 345 continuous accumulation of volatile fatty acids (He et al., 2022). The results showed that the  
39  
40  
41 346 pH decreased continuously after the AD started and reached the lowest value on the 5th day.  
42  
43  
44 347 The redox potential of the AD system can affect the microbial growth activities, and low  
45  
46  
47 348 redox potential means more strict anaerobic conditions and stronger reduction (Xu et al.,  
48  
49  
50 349 2014). Methane production requires the consumption of reducible substances. The  
51  
52  
53 350 breakdown of organic matter caused an initial increase in TOC content of the liquid phase,  
54  
55  
56 351 which then declined as methanogens utilized these materials to produce methane. The  
57  
58  
59 352 Pearson correlation analyses also revealed that these parameters were correlated with biogas  
60  
61 353 yields (Fig. S5).  
62  
63  
64  
65

1 354 Although the biogas production differed considerably between different DC, the  
2  
3  
4 355 methane content of these biogas did not vary greatly, with an overall value of around 60%  
5  
6 356 (Fig. 5). According to the final measurements, the highest values of net methane yield were  
7  
8  
9 357 found in the DC3 or DC4 samples after 35 d, with 134.76 and 142.51 mL/g VS for the Birch  
10  
11  
12 358 DC3 and Ash DC4 samples, respectively. The theoretical methane production, calculated by  
13  
14  
15 359 the elemental composition using the Buswell formula, did not differ significantly between  
16  
17  
18 360 different DC (Table S3). Therefore, the biodegradability index corresponded to the total  
19  
20  
21 361 biogas yield results, with DC3 samples being the highest and DC1 samples the lowest. The  
22  
23  
24 362 degradation of wood in the forest did not significantly change its elemental (carbon, hydrogen,  
25  
26  
27 363 oxygen, and nitrogen) composition (Table 2). However, due to the extremely low content of  
28  
29  
30 364 nitrogen in fresh wood, a slight increase in nitrogen can significantly shift the carbon to  
31  
32  
33 365 nitrogen ratio, making the samples more applicable to AD.

### 366 3.4 The fitting and prediction of methane yield

39 367 To investigate the methanogenic kinetics, a modified Gompertz model was employed to  
40  
41  
42 368 fit the cumulative biogas yield curves, and the kinetic parameters of fitting results are shown  
43  
44  
45 369 in Table S4. The lag period is a parameter that reflects the adaptation of microbes to the AD  
46  
47  
48 370 system during the initial stage (Mao et al., 2017). As shown in Table S4, the DC3 digesters  
49  
50  
51 371 had the shortest lag period, which is attributed to these samples having the highest WEOC  
52  
53  
54 372 content, being rapidly hydrolyzed and converted to methane. It can be seen that the maximum  
55  
56  
57 373 biogas potential corresponds quite well to the experimental values. In addition, the maximum  
58  
59  
60 374 specific biogas production rate of digester DC3 and DC4 samples were noticeably higher

1 375 than that of other digesters, which was in good agreement with the experimental results.

2  
3 376 Overall, all cumulative biogas yield curves can be well fitted by the modified Gompertz

4  
5  
6 377 model, and the correlation coefficient of fitting results was between 0.95 and 0.99.

7  
8  
9 378 Prior to performing AD, it is desirable to determine the optimal parameters for maximum

10  
11  
12 379 methane yield from woody waste. To the best of our knowledge, an approach that can predict

13  
14  
15 380 methane yield from woody waste while addressing the issues involved in identifying the

16  
17  
18 381 optimal digestion conditions and feedstock properties to maximize methane yield has not yet

19  
20  
21 382 been developed. As shown in Table S3, the random forest model predicted biogas production

22  
23  
24 383 well with an error rate of around 25%. The machine learning model (random forest)

25  
26  
27 384 prediction accuracies of some samples were close to the results of the Gompertz fitting,

28  
29  
30 385 indicating that the machine learning model is instructive in practical AD with woody waste.

31  
32  
33 386 It is worth noting that the predictions for the Birch DC1 samples were less accurate. This

34  
35  
36 387 may be because the previously established database for creating machine learning models

37  
38  
39 388 was not comprehensive and lacked data on this part of relatively low methane production

40  
41  
42 389 (Gao et al., 2024a). Therefore, more experiments on AD of woody biomass are needed in the

43  
44  
45 390 future in order to expand the database for improving the model.

### 46 47 391 3.5 Applications and Future considerations

48  
49  
50 392 The present study introduces a novel nature-based approach to enhance suitability of

51  
52  
53 393 wood waste, particularly forest residues, for AD, providing a sustainable solution to two key

54  
55  
56 394 issues that have hampered the practical application of wood waste AD. Firstly, the low

57  
58  
59 395 methane production from wood has been overcome with an average increase of 160% in

1 396 methane yield after this nature-based approach (DC3 compared to DC1). This is comparable  
2  
3  
4 397 to other, more intensive, pretreatment technologies such as combined  
5  
6 398 hydrothermal/enzymatic treatment (168% improvement) (Matsakas et al., 2015), aqueous  
7  
8  
9 399 ammonia soaking (151% improvement) (Antonopoulou et al., 2015), or combined ethanol  
10  
11  
12 400 organosolve/hydrothermal treatment (194% improvement) (Charnnok et al., 2020). Secondly,  
13  
14  
15 401 the lack of economical pretreatment technologies further hindered the practical utilization of  
16  
17  
18 402 wood waste AD. The proposed method leverages natural systems without requiring  
19  
20  
21 403 significant additional economic inputs, with the potential to be highly cost-effective as a  
22  
23  
24 404 result. By harnessing the inherent capabilities of natural forest processes, this nature-based  
25  
26  
27 405 approach offers a practical and scalable solution for enhancing the efficiency of AD  
28  
29  
30 406 operations for wood waste.

31  
32 407 The economic viability of AD with wood waste has been thoroughly described in the  
33  
34  
35 408 literature. Teghammar et al. (2014) conducted an economic assessment of biogas production  
36  
37  
38 409 from forest residues with pretreatment enhancement, showing that an AD plant processing  
39  
40  
41 410 50000 tons dry weight of forest residues per year is economically viable. The techno-  
42  
43  
44 411 economic assessment showed that methanol pretreatment was more financially acceptable  
45  
46  
47 412 than acetic acid and ethanol, and the capital investment for operating an AD plant treating  
48  
49  
50 413 20,000 tons of forest residues per year could be recouped within eight years (Kabir et al.,  
51  
52  
53 414 2015). Moreover, AD was shown to be an environmentally friendly method of recovering  
54  
55  
56 415 energy from wood waste compared to other management processes through life cycle  
57  
58  
59 416 assessment analysis (da Costa et al., 2020; Liang et al., 2017; Nogueira et al., 2021). To  
60  
61 417 further explore the differences between all DC samples and find the best DC for application  
62  
63  
64  
65

1 418 in AD, a net profit analysis was conducted. Considering that the AD process was the same  
2  
3  
4 419 for all DC samples, the net energy output could be calculated from the electricity input of  
5  
6 420 grinding the samples and the methane production. According to Wu et al. (2016), the calorific  
7  
8  
9 421 value of methane is 11.06 kWh/m<sup>3</sup>. As shown in Fig. 6, DC3 had a high net energy output,  
10  
11  
12 422 which implies that this stage has the potential to be used in AD plants. For fire protection  
13  
14  
15 423 reasons and energy considerations, the forest residues should not be retained in the forest.  
16  
17  
18 424 Unfortunately, the direct recycling of these forest residues also may result in the removal of  
19  
20  
21 425 minerals that would otherwise fertilize the soil and promote the future growth of trees  
22  
23  
24 426 (Grotsky et al., 2018). These results may provide guidance on specific collection times for  
25  
26  
27 427 forest residues in practice. This study proposes to collect DC3 samples, which satisfies the  
28  
29  
30 428 requirement of releasing minerals from the wood waste to maintain the forest ecology while  
31  
32  
33 429 keeping the highest methane yield.

35 430 To better utilize this nature-based approach, more detailed experiments and analyses are  
36  
37  
38 431 still needed to bridge the following issues. Firstly, more wood samples of various species are  
39  
40  
41 432 needed to verify the generalizability of this approach, as well as to investigate the duration  
42  
43  
44 433 for forest residues to reach DC3 in different forest environments to facilitate the collection  
45  
46  
47 434 of samples. Secondly, there is a loss of mass in the degradation process of forest residues  
48  
49  
50 435 (Oberle et al., 2020; Seibold et al., 2021), so it is important to explore how mass loss varies  
51  
52  
53 436 with DC. Thirdly, anaerobic co-digestion of wood waste with other organic wastes can  
54  
55  
56 437 balance the carbon to nitrogen ratio of the substrate and enhance methane production (Li et  
57  
58  
59 438 al., 2019; Oh et al., 2018). Additionally, the combination of other pretreatment technologies  
60  
61  
62 439 can improve substrate availability to microorganisms in AD (Wang et al., 2024; Zhang et al.,

1 440 2017). Therefore, anaerobic co-digestion of different DC wood waste and other organic  
2  
3  
4 441 wastes and the possibility of combining this nature-based approach with other pretreatments  
5  
6 442 need to be explored for maximizing energy recovery from wood wastes.  
7  
8

## 9 443 **4 Conclusion**

10  
11  
12 444 This study investigated a novel nature-based approach to promote AD application of  
13  
14  
15 445 forest residues. Specifically, this approach exploited the lignocellulose degradation processes  
16  
17  
18 446 inherent in forest ecosystems, combined with a strategic collection to maximize the AD  
19  
20  
21 447 potential of forest residues. Based on the experimental results, the following conclusions can  
22  
23  
24 448 be drawn:

- 25  
26 449 1) The texture of the forest residues was softened by processing with this nature-based  
27  
28  
29 450 approach, making them easier to be shredded. The SEC results showed that the energy  
30  
31  
32 451 required to grind the same dry weight of wood sample decreased with increasing DC.  
33  
34  
35 452 A subsequent particle size analysis showed that wood samples with higher DC had  
36  
37  
38 453 smaller average particle sizes after grinding.
- 39  
40  
41 454 2) High DC wood samples had higher WEOC, lower cellulose crystallinity, and a more  
42  
43  
44 455 suitable carbon to nitrogen ratio for AD. Although the lignin content was relatively  
45  
46  
47 456 higher in high DC wood samples, the recalcitrance of their lignocellulosic structure  
48  
49  
50 457 was disrupted. These changes are expected to lead to enhanced methane production  
51  
52  
53 458 because of a breakdown of the lignocellulosic structure, increasing access to  
54  
55  
56 459 microorganisms involved in AD.
- 57  
58 460 3) A preliminary test of this nature-based approach by AD experiments showed that  
59  
60  
61 461 wood samples from DC 1 had the lowest methane yield, while DC 3 samples had the

1 462 highest, with a notable 160% increase compared to DC 1. In addition, the net profit  
2  
3  
4 463 analysis indicated that wood samples from DC 3 to DC 5 had a net energy output  
5  
6 464 when applied in AD, with the net energy output being relatively high in DC 3 and DC  
7  
8  
9 465 4. Therefore, these results imply that DC3 might be the optimal level of decay for  
10  
11  
12 466 forest residues collection.  
13

14  
15 467 This study is the first to introduce the concept of a nature-based approach to enhance the  
16  
17  
18 468 AD performance of forest residues, and to explore it in detail experimentally. This approach,  
19  
20  
21 469 when combined with a strategic collection method, can significantly improve the overall  
22  
23  
24 470 profitability and sustainability of bioenergy production from forest residues. Furthermore,  
25  
26  
27 471 the feasibility of more forest ecosystems in boosting the AD application of forest residues  
28  
29  
30 472 should be further explored, as this can broaden the applications of this novel nature-based  
31  
32  
33 473 approach.  
34

## 35 474 **Acknowledgments**

36  
37  
38 475 The authors gratefully acknowledge financial support from the China Scholarship  
39  
40  
41 476 Council (CSC) for Zhenghui Gao (CSC No. 202006760088). Sapsford, Cleall and Harbottle  
42  
43  
44 477 were supported by the UK Research and Innovation-funded project ‘ASPIRE – Accelerated  
45  
46  
47 478 Supergene Processes in Repository Engineering’ (EP/T03100X/1).  
48

## 49 479 **Reference**

50  
51  
52 480 Alexandropoulou, M., Antonopoulou, G., Ntaikou, I., Lyberatos, G., 2017. Fungal Pretreatment of Willow  
53 481 Sawdust with *Abortiporus biennis* for Anaerobic Digestion: Impact of an External Nitrogen Source.  
54 482 Sustainability 9, 130. <https://doi.org/10.3390/su9010130>  
55  
56 483 Ali, S.S., Abomohra, A.E.-F., Sun, J., 2017. Effective bio-pretreatment of sawdust waste with a novel microbial  
57 484 consortium for enhanced biomethanation. Bioresour. Technol. 238, 425–432.  
58  
59 485 <https://doi.org/10.1016/j.biortech.2017.03.187>  
60  
61  
62  
63  
64  
65

- 1 486 Antonopoulou, G., Gavala, H.N., Skiadas, I.V., Lyberatos, G., 2015. The Effect of Aqueous Ammonia Soaking  
2 487 Pretreatment on Methane Generation Using Different Lignocellulosic Biomasses. *Waste Biomass*  
3 488 *Valorization* 6, 281–291. <https://doi.org/10.1007/s12649-015-9352-9>
- 4 489 Atelge, M.R., Atabani, A.E., Banu, J.R., Krisa, D., Kaya, M., Eskicioglu, C., Kumar, G., Lee, C., Yildiz, Y.Ş.,  
5 490 Unalan, S., Mohanasundaram, R., Duman, F., 2020. A critical review of pretreatment technologies to  
6 491 enhance anaerobic digestion and energy recovery. *Fuel* 270, 117494.  
7 492 <https://doi.org/10.1016/j.fuel.2020.117494>
- 8 493 Awoyale, A.A., Lokhat, D., 2021. Experimental determination of the effects of pretreatment on selected  
9 494 Nigerian lignocellulosic biomass in bioethanol production. *Sci. Rep.* 11, 557.  
10 495 <https://doi.org/10.1038/s41598-020-78105-8>
- 11 496 Charnnok, B., Sawangkeaw, R., Chaiprapat, S., 2020. Integrated process for the production of fermentable sugar  
12 497 and methane from rubber wood. *Bioresour. Technol.* 302, 122785.  
13 498 <https://doi.org/10.1016/j.biortech.2020.122785>
- 14 499 D' Silva, T.C., Isha, A., Verma, S., Shirsath, G., Chandra, R., Vijay, V.K., Subbarao, P.M.V., Kovács, K.L.,  
15 500 2022. Anaerobic co-digestion of dry fallen leaves, fruit/vegetable wastes and cow dung without an  
16 501 active inoculum – A biomethane potential study. *Bioresour. Technol. Rep.* 19, 101189.  
17 502 <https://doi.org/10.1016/j.biteb.2022.101189>
- 18 503 da Costa, T.P., Quinteiro, P., Arroja, L., Dias, A.C., 2020. Environmental comparison of forest biomass residues  
19 504 application in Portugal: Electricity, heat and biofuel. *Renew. Sustain. Energy Rev.* 134, 110302.  
20 505 <https://doi.org/10.1016/j.rser.2020.110302>
- 21 506 Dai, B., Guo, X., Yuan, D., Xu, J., 2018. Comparison of Different Pretreatments of Rice Straw Substrate to  
22 507 Improve Biogas Production. *Waste Biomass Valorization* 9, 1503–1512.  
23 508 <https://doi.org/10.1007/s12649-017-9950-9>
- 24 509 Dai, X., Hua, Y., Dai, L., Cai, C., 2019. Particle size reduction of rice straw enhances methane production under  
25 510 anaerobic digestion. *Bioresour. Technol.* 293, 122043. <https://doi.org/10.1016/j.biortech.2019.122043>
- 26 511 Darmawan, S., Wistara, N.J., Pari, G., Maddu, A., Syafii, W., 2016. Characterization of Lignocellulosic  
27 512 Biomass as Raw Material for the Production of Porous Carbon-based Materials. *BioResources* 11,  
28 513 3561–3574.
- 29 514 Díez, D., Urueña, A., Piñero, R., Barrio, A., Tamminen, T., 2020. Determination of Hemicellulose, Cellulose,  
30 515 and Lignin Content in Different Types of Biomasses by Thermogravimetric Analysis and  
31 516 Pseudocomponent Kinetic Model (TGA-PKM Method). *Processes* 8, 1048.  
32 517 <https://doi.org/10.3390/pr8091048>
- 33 518 Eom, T., Chaiprapat, S., Charnnok, B., 2019. Enhanced enzymatic hydrolysis and methane production from  
34 519 rubber wood waste using steam explosion. *J. Environ. Manage.* 235, 231–239.  
35 520 <https://doi.org/10.1016/j.jenvman.2019.01.041>
- 36 521 Gao, Z., Alshehri, K., Li, Y., Qian, H., Sapsford, D., Cleall, P., Harbottle, M., 2022. Advances in biological  
37 522 techniques for sustainable lignocellulosic waste utilization in biogas production. *Renew. Sustain.*  
38 523 *Energy Rev.* 170, 112995. <https://doi.org/10.1016/j.rser.2022.112995>
- 39 524 Gao, Z., Cui, T., Qian, H., Sapsford, D.J., Cleall, P.J., Harbottle, M.J., 2024a. Can wood waste be a feedstock  
40 525 for anaerobic digestion? A machine learning assisted *meta-analysis*. *Chem. Eng. J.* 150496.  
41 526 <https://doi.org/10.1016/j.cej.2024.150496>
- 42 527 Gao, Z., Muaaz-Us-Salam, S., Sapsford, D., Cleall, P., Harbottle, M., 2023. Application of natural  
43 528 biodelignification systems in forest soil for enhanced anaerobic digestion potential of wood waste.

- 529 Presented at the Proceedings of the 9th International Congress on Environmental Geotechnics  
1 530 (ICEG2023), pp. 13–22. <https://doi.org/10.53243/ICEG2023-59>
- 2  
3 531 Gao, Z., Qian, H., Cui, T., Ren, Z., Wang, X., 2024b. Comprehensive *meta*-analysis reveals the impact of non-  
4 532 biodegradable plastic pollution on methane production in anaerobic digestion. *Chem. Eng. J.* 484,  
5 533 149703. <https://doi.org/10.1016/j.cej.2024.149703>
- 6  
7 534 Gao, Z., Ren, Z., Cui, T., Fu, Y., 2025. Machine learning-based analysis of microplastic-induced changes in  
8 535 anaerobic digestion parameters influencing methane yield. *J. Environ. Manage.* 377, 124627.  
9 536 <https://doi.org/10.1016/j.jenvman.2025.124627>
- 10  
11 537 Garvie, L.C., Roxburgh, S.H., Ximenes, F.A., 2021. Greenhouse Gas Emission Offsets of Forest Residues for  
12 538 Bioenergy in Queensland, Australia. *Forests* 12, 1570. <https://doi.org/10.3390/f12111570>
- 13  
14 539 Grodsky, S.M., Moorman, C.E., Fritts, S.R., Campbell, J.W., Sorenson, C.E., Bertone, M.A., Castleberry, S.B.,  
15 540 Wigley, T.B., 2018. Invertebrate community response to coarse woody debris removal for bioenergy  
16 541 production from intensively managed forests. *Ecol. Appl.* 28, 135–148.  
17 542 <https://doi.org/10.1002/eap.1634>
- 18  
19 543 Hashemi, S., Solli, L., Aasen, R., Lamb, J.J., Horn, S.J., Lien, K.M., 2022. Stimulating biogas production from  
20 544 steam-exploded birch wood using Fenton reaction and fungal pretreatment. *Bioresour. Technol.* 366,  
21 545 128190. <https://doi.org/10.1016/j.biortech.2022.128190>
- 22  
23 546 He, C., Song, H., Liu, L., Li, P., Kumar Awasthi, M., Xu, G., Zhang, Q., Jiao, Y., Chang, C., Yang, Y., 2022.  
24 547 Enhancement of methane production by anaerobic digestion of corn straw with hydrogen-nanobubble  
25 548 water. *Bioresour. Technol.* 344, 126220. <https://doi.org/10.1016/j.biortech.2021.126220>
- 26  
27 549 Isha, A., D' Silva, T.C., Subbarao, P.M.V., Chandra, R., Vijay, V.K., 2021. Stabilization of anaerobic digestion  
28 550 of kitchen wastes using protein-rich additives: Study of process performance, kinetic modelling and  
29 551 energy balance. *Bioresour. Technol.* 337, 125331. <https://doi.org/10.1016/j.biortech.2021.125331>
- 30  
31 552 Ji, J.-L., Chen, F., Liu, S., Yang, Y., Hou, C., Wang, Y.-Z., 2022. Co-production of biogas and humic acid using  
32 553 rice straw and pig manure as substrates through solid-state anaerobic fermentation and subsequent  
33 554 aerobic composting. *J. Environ. Manage.* 320, 115860.  
34 555 <https://doi.org/10.1016/j.jenvman.2022.115860>
- 35  
36 556 Kabir, M.M., Rajendran, K., Taherzadeh, M.J., Sárvári Horváth, I., 2015. Experimental and economical  
37 557 evaluation of bioconversion of forest residues to biogas using organosolv pretreatment. *Bioresour.*  
38 558 *Technol.* 178, 201–208. <https://doi.org/10.1016/j.biortech.2014.07.064>
- 39  
40 559 Kamarudin, S.N.C., Jainal, M.S., Azizan, A., Safaai, N.S.M., Daud, A.R.M., 2014. Mechanical Pretreatment  
41 560 of Lignocellulosic Biomass for Biofuel Production. *Appl. Mech. Mater.* 625, 838–841.  
42 561 <https://doi.org/10.4028/www.scientific.net/AMM.625.838>
- 43  
44 562 Karami, K., Karimi, K., Mirmohamadsadeghi, S., Kumar, R., 2022. Mesophilic aerobic digestion: An efficient  
45 563 and inexpensive biological pretreatment to improve biogas production from highly-recalcitrant  
46 564 pinewood. *Energy* 239, 122361. <https://doi.org/10.1016/j.energy.2021.122361>
- 47  
48 565 Kumar, S., D' Silva, T.C., Chandra, R., Malik, A., Vijay, V.K., Misra, A., 2021. Strategies for boosting  
49 566 biomethane production from rice straw: A systematic review. *Bioresour. Technol. Rep.* 15, 100813.  
50 567 <https://doi.org/10.1016/j.biteb.2021.100813>
- 51  
52 568 Kumar, S., Gandhi, P., Yadav, M., Paritosh, K., Pareek, N., Vivekanand, V., 2019. Weak alkaline treatment of  
53 569 wheat and pearl millet straw for enhanced biogas production and its economic analysis. *Renew. Energy*  
54 570 139, 753–764. <https://doi.org/10.1016/j.renene.2019.02.133>

- 571 Kurvits, V., Ots, K., Kangur, A., Korjus, H., Muiste, P., 2020. Assessment of load and quality of logging  
572 residues from clear-felling areas in Järvselja: a case study from Southeast Estonia. *Cent. Eur. For. J.*  
573 66, 3–11. <https://doi.org/10.2478/forj-2019-0022>
- 574 Lai, Z., Chen, D., Jiang, E., Zhao, L., Vallejo, L.E., Zhou, W., 2021. Effect of fractal particle size distribution  
575 on the mobility of dry granular flows. *AIP Adv.* 11, 095113. <https://doi.org/10.1063/5.0065051>
- 576 Lee, E., Han, H.-S., 2017. Air Curtain Burners: A Tool for Disposal of Forest Residues. *Forests* 8, 296.  
577 <https://doi.org/10.3390/f8080296>
- 578 Li, R., Tan, W., Zhao, X., Dang, Q., Song, Q., Xi, B., Zhang, X., 2019. Evaluation on the Methane Production  
579 Potential of Wood Waste Pretreated with NaOH and Co-Digested with Pig Manure. *Catalysts* 9, 539.  
580 <https://doi.org/10.3390/catal9060539>
- 581 Liang, S., Gu, H., Bergman, R.D., 2017. Life cycle assessment of cellulosic ethanol and biomethane production  
582 from forest residues. *BioResources* 12, 7873–7883. <https://doi.org/10.15376/biores.12.4.7873-7883>
- 583 Liu, X., Hilgsmann, S., Gourdon, R., Bayard, R., 2017. Anaerobic digestion of lignocellulosic biomasses  
584 pretreated with *Ceriporiopsis subvermispora*. *J. Environ. Manage.* 193, 154–162.  
585 <https://doi.org/10.1016/j.jenvman.2017.01.075>
- 586 Liu, X., Zicari, S.M., Liu, G., Li, Y., Zhang, R., 2015. Pretreatment of wheat straw with potassium hydroxide  
587 for increasing enzymatic and microbial degradability. *Bioresour. Technol.* 185, 150–157.  
588 <https://doi.org/10.1016/j.biortech.2015.02.047>
- 589 Lübken, M., Gehring, T., Wichern, M., 2010. Microbiological fermentation of lignocellulosic biomass: current  
590 state and prospects of mathematical modeling. *Appl. Microbiol. Biotechnol.* 85, 1643–1652.  
591 <https://doi.org/10.1007/s00253-009-2365-1>
- 592 Luo, L., Qu, Y., Gong, W., Qin, L., Li, W., Sun, Y., 2021. Effect of Particle Size on the Aerobic and Anaerobic  
593 Digestion Characteristics of Whole Rice Straw. *Energies* 14, 3960.  
594 <https://doi.org/10.3390/en14133960>
- 595 Manikandan, S., Vickram, S., Sirohi, R., Subbaiya, R., Krishnan, R.Y., Karmegam, N., Sumathijones, C.,  
596 Rajagopal, R., Chang, S.W., Ravindran, B., Awasthi, M.K., 2023. Critical review of biochemical  
597 pathways to transformation of waste and biomass into bioenergy. *Bioresour. Technol.* 372, 128679.  
598 <https://doi.org/10.1016/j.biortech.2023.128679>
- 599 Mao, C., Wang, X., Xi, J., Feng, Y., Ren, G., 2017. Linkage of kinetic parameters with process parameters and  
600 operational conditions during anaerobic digestion. *Energy* 135, 352–360.  
601 <https://doi.org/10.1016/j.energy.2017.06.050>
- 602 Matsakas, L., Rova, U., Christakopoulos, P., 2015. Sequential parametric optimization of methane production  
603 from different sources of forest raw material. *Front. Microbiol.* 6.
- 604 Miao, Z., Grift, T.E., Hansen, A.C., Ting, K.C., 2011. Energy requirement for comminution of biomass in  
605 relation to particle physical properties. *Ind. Crops Prod.* 33, 504–513.  
606 <https://doi.org/10.1016/j.indcrop.2010.12.016>
- 607 Mo, X., Wang, M., Wang, Y., Zhang, P., Zhang, A., Kong, D., Zeng, H., Wang, J., 2022. High content and  
608 distinct spectroscopic characteristics of water-extractable organic matter in rhizosphere soils in a  
609 semiarid grassland. *Rhizosphere* 23, 100553. <https://doi.org/10.1016/j.rhisph.2022.100553>
- 610 Mohsenzadeh, A., Jeihanipour, A., Karimi, K., Taherzadeh, M.J., 2012. Alkali pretreatment of softwood spruce  
611 and hardwood birch by NaOH/thiourea, NaOH/urea, NaOH/urea/thiourea, and NaOH/PEG to improve  
612 ethanol and biogas production. *J. Chem. Technol. Biotechnol.* 87, 1209–1214.  
613 <https://doi.org/10.1002/jctb.3695>

- 614 Moiceanu, G., Paraschiv, G., Voicu, G., Dinca, M., Negoita, O., Chitoiu, M., Tudor, P., 2019. Energy  
615 Consumption at Size Reduction of Lignocellulose Biomass for Bioenergy. *Sustainability* 11, 2477.  
616 <https://doi.org/10.3390/su11092477>
- 617 Molenda, M., Horabik, J., Parafiniuk, P., Oniszczuk, A., Bańda, M., Wajs, J., Gondek, E., Chutkowski, M.,  
618 Lisowski, A., Wiącek, J., Stasiak, M., 2021. Mechanical and Combustion Properties of Agglomerates  
619 of Wood of Popular Eastern European Species. *Materials* 14, 2728.  
620 <https://doi.org/10.3390/ma14112728>
- 621 Muaz-Us-Salam, S., Cleall, P.J., Harbottle, M.J., 2020. Application of enzymatic and bacterial  
622 biodelignification systems for enhanced breakdown of model lignocellulosic wastes. *Sci. Total*  
623 *Environ.* 728, 138741. <https://doi.org/10.1016/j.scitotenv.2020.138741>
- 624 Mulat, D.G., Huerta, S.G., Kalyani, D., Horn, S.J., 2018. Enhancing methane production from lignocellulosic  
625 biomass by combined steam-explosion pretreatment and bioaugmentation with cellulolytic bacterium  
626 *Caldicellulosiruptor bescii*. *Biotechnol. Biofuels* 11, 19. <https://doi.org/10.1186/s13068-018-1025-z>
- 627 Nicholls, D.L., Halbrook, J.M., Benedum, M.E., Han, H.-S., Lowell, E.C., Becker, D.R., Barbour, R.J., 2018.  
628 Socioeconomic Constraints to Biomass Removal from Forest Lands for Fire Risk Reduction in the  
629 Western U.S. *Forests* 9, 264. <https://doi.org/10.3390/f9050264>
- 630 Nogueira, G.P., McManus, M.C., Leak, D.J., Franco, T.T., Oliveira de Souza Dias, M., Nakao Cavaliero, C.K.,  
631 2021. Are eucalyptus harvest residues a truly burden-free biomass source for bioenergy? A deeper  
632 look into biorefinery process design and Life Cycle Assessment. *J. Clean. Prod.* 299, 126956.  
633 <https://doi.org/10.1016/j.jclepro.2021.126956>
- 634 Oberle, B., Lee, M.R., Myers, J.A., Osazuwa-Peters, O.L., Spasojevic, M.J., Walton, M.L., Young, D.F., Zanne,  
635 A.E., 2020. Accurate forest projections require long-term wood decay experiments because plant trait  
636 effects change through time. *Glob. Change Biol.* 26, 864–875. <https://doi.org/10.1111/gcb.14873>
- 637 Oh, J.-I., Lee, J., Lin, K.-Y.A., Kwon, E.E., Fai Tsang, Y., 2018. Biogas production from food waste via  
638 anaerobic digestion with wood chips. *Energy Environ.* 29, 1365–1372.  
639 <https://doi.org/10.1177/0958305X18777234>
- 640 Pergola, M.T., Saulino, L., Castellaneta, M., Rita, A., Pecora, G., Cozzi, M., Moretti, N., Pericolo, O., Pierangeli,  
641 D., Romano, S., Viccaro, M., Ripullone, F., 2022. Towards sustainable management of forest residues  
642 in the southern Apennine Mediterranean mountain forests: a scenario-based approach. *Ann. For. Sci.*  
643 79, 14. <https://doi.org/10.1186/s13595-022-01128-w>
- 644 Petritan, I.C., Mihăilă, V.-V., Yuste, J.C., Bouriaud, O., Petritan, A.M., 2023. Deadwood density, C stocks and  
645 their controlling factors in a beech-silver fir mixed virgin European forest. *For. Ecol. Manag.* 539,  
646 121007. <https://doi.org/10.1016/j.foreco.2023.121007>
- 647 Piątek, M., Lisowski, A., Kasprzycka, A., Lisowska, B., 2016. The dynamics of an anaerobic digestion of crop  
648 substrates with an unfavourable carbon to nitrogen ratio. *Bioresour. Technol.* 216, 607–612.  
649 <https://doi.org/10.1016/j.biortech.2016.05.122>
- 650 Provenzano, M.R., Malerba, A.D., Pezzolla, D., Gigliotti, G., 2014. Chemical and spectroscopic  
651 characterization of organic matter during the anaerobic digestion and successive composting of pig  
652 slurry. *Waste Manag.* 34, 653–660. <https://doi.org/10.1016/j.wasman.2013.12.001>
- 653 Rabot, E., Wiesmeier, M., Schlüter, S., Vogel, H.-J., 2018. Soil structure as an indicator of soil functions: A  
654 review. *Geoderma* 314, 122–137. <https://doi.org/10.1016/j.geoderma.2017.11.009>
- 655 Rego, F., Soares Dias, A.P., Casquilho, M., Rosa, F.C., Rodrigues, A., 2019. Fast determination of  
656 lignocellulosic composition of poplar biomass by thermogravimetry. *Biomass Bioenergy* 122, 375–  
657 380. <https://doi.org/10.1016/j.biombioe.2019.01.037>

- 658 Rice, E.W., Baird, R.B., Eaton, A.D., 2017. Standard Methods for the Examination of Water and Wastewater,  
659 23rd edn. American Public Health Association, American Water Works Association, Water  
660 Environment Federation (2017). ISBN: 9780875532875.
- 661 Salehian, P., Karimi, K., Zilouei, H., Jeihanipour, A., 2013. Improvement of biogas production from pine wood  
662 by alkali pretreatment. *Fuel* 106, 484–489. <https://doi.org/10.1016/j.fuel.2012.12.092>
- 663 Seibold, S., Rammer, W., Hothorn, T., Seidl, R., Ulyshen, M.D., Lorz, J., Cadotte, M.W., Lindenmayer, D.B.,  
664 Adhikari, Y.P., Aragón, R., Bae, S., Baldrian, P., Barimani Varandi, H., Barlow, J., Bässler, C.,  
665 Beauchêne, J., Berenguer, E., Bergamin, R.S., Birkemoe, T., Boros, G., Brandl, R., Brustel, H., Burton,  
666 P.J., Cakpo-Tossou, Y.T., Castro, J., Cateau, E., Cobb, T.P., Farwig, N., Fernández, R.D., Firn, J., Gan,  
667 K.S., González, G., Gossner, M.M., Habel, J.C., Hébert, C., Heibl, C., Heikkala, O., Hemp, A., Hemp,  
668 C., Hjältén, J., Hotes, S., Kouki, J., Lachat, T., Liu, J., Liu, Y., Luo, Y.-H., Macandog, D.M., Martina,  
669 P.E., Mukul, S.A., Nachin, B., Nisbet, K., O’Halloran, J., Oxbrough, A., Pandey, J.N., Pavlíček, T.,  
670 Pawson, S.M., Rakotondranary, J.S., Ramanamanjato, J.-B., Rossi, L., Schmidl, J., Schulze, M.,  
671 Seaton, S., Stone, M.J., Stork, N.E., Suran, B., Sverdrup-Thygeson, A., Thorn, S., Thyagarajan, G.,  
672 Wardlaw, T.J., Weisser, W.W., Yoon, S., Zhang, N., Müller, J., 2021. The contribution of insects to  
673 global forest deadwood decomposition. *Nature* 597, 77–81. <https://doi.org/10.1038/s41586-021-03740-8>
- 674
- 675 Shorohova, E., Kapitsa, E., Kuznetsov, A., Kuznetsova, S., Lopes de Gerenuy, V., Kaganov, V., Kurganova, I.,  
676 2021. Decay classes of coarse woody debris in a lowland Dipterocarp forest: implications for volume,  
677 density, and carbon estimates. *Biotropica* 53, 879–887. <https://doi.org/10.1111/btp.12947>
- 678 Song, C., Cai, F., Yang, S., Wang, L., Liu, G., Chen, C., 2024. Machine learning-based prediction of methane  
679 production from lignocellulosic wastes. *Bioresour. Technol.* 393, 129953.  
680 <https://doi.org/10.1016/j.biortech.2023.129953>
- 681 Tarasov, D., Leitch, M., Fatehi, P., 2018. Lignin–carbohydrate complexes: properties, applications, analyses,  
682 and methods of extraction: a review. *Biotechnol. Biofuels* 11, 269. [https://doi.org/10.1186/s13068-](https://doi.org/10.1186/s13068-018-1262-1)  
683 018-1262-1
- 684 Tatti, D., Fatton, V., Sartori, L., Gobat, J.-M., Le Bayon, R.-C., 2018. What does ‘lignoform’ really mean? *Appl.*  
685 *Soil Ecol., HUMUSICA* 3 - Reviews, Applications, Tools 123, 632–645.  
686 <https://doi.org/10.1016/j.apsoil.2017.06.037>
- 687 Teghammar, A., Forgács, G., Sárvári Horváth, I., Taherzadeh, M.J., 2014. Techno-economic study of NMMO  
688 pretreatment and biogas production from forest residues. *Appl. Energy* 116, 125–133.  
689 <https://doi.org/10.1016/j.apenergy.2013.11.053>
- 690 Tian, Y., Zhang, H., Mi, X., Wang, L., Zhang, L., Ai, Y., 2016. Research on anaerobic digestion of corn stover  
691 enhanced by dilute acid pretreatment: Mechanism study and potential utilization in practical  
692 application. *J. Renew. Sustain. Energy* 8, 023103. <https://doi.org/10.1063/1.4945570>
- 693 Wang, W., Jiang, M.-F., Hsu, J.-R., Guo, G.-L., 2024. Integrated alkaline-solid/liquid separation-thermal  
694 multiple-step pretreatment of lignocellulosic biomass for biogas production enhancement. *Biomass*  
695 *Convers. Biorefinery*. <https://doi.org/10.1007/s13399-024-05288-9>
- 696 Wang, Z.-W., Xu, F., Manchala, K.R., Sun, Y., Li, Y., 2016. Fractal-like kinetics of the solid-state anaerobic  
697 digestion. *Waste Manag.* 53, 55–61. <https://doi.org/10.1016/j.wasman.2016.04.019>
- 698 Wu, A., Lovett, D., McEwan, M., Cecelja, F., Chen, T., 2016. A spreadsheet calculator for estimating biogas  
699 production and economic measures for UK-based farm-fed anaerobic digesters. *Bioresour. Technol.*  
700 220, 479–489. <https://doi.org/10.1016/j.biortech.2016.08.103>

1 701 Xing, M., Li, X., Yang, J., Huang, Z., Lu, Y., 2012. Changes in the chemical characteristics of water-extracted  
2 702 organic matter from vermicomposting of sewage sludge and cow dung. *J. Hazard. Mater.* 205–206,  
3 703 24–31. <https://doi.org/10.1016/j.jhazmat.2011.11.070>  
4 704 Xu, S., Selvam, A., Wong, J.W.C., 2014. Optimization of micro-aeration intensity in acidogenic reactor of a  
5 705 two-phase anaerobic digester treating food waste. *Waste Manag.* 34, 363–369.  
6 706 <https://doi.org/10.1016/j.wasman.2013.10.038>  
7 707 Xu, W., Fu, S., Yang, Z., Lu, J., Guo, R., 2018. Improved methane production from corn straw by microaerobic  
8 708 pretreatment with a pure bacteria system. *Bioresour. Technol.* 259, 18–23.  
9 709 <https://doi.org/10.1016/j.biortech.2018.02.046>  
10 710 Yoon, S.-M., Kim, M.-J., Hwang, W.-J., Lee, H.-M., Park, Y., Son, D.-W., Kim, Y.-S., Choi, Y.-S., 2023.  
11 711 Natural durability and fungal diversity of five wood species in a field-test site in Jeongseon, Korea.  
12 712 *Holzforschung* 77, 577–584. <https://doi.org/10.1515/hf-2023-0034>  
13 713 Zhang, B., Ji, M., Wang, F., Li, R., Zhang, K., Yin, X., Li, Q., 2017. Damage of EPS and cell structures and  
14 714 improvement of high-solid anaerobic digestion of sewage sludge by combined (Ca(OH)<sub>2</sub> + multiple-  
15 715 transducer ultrasonic) pretreatment. *RSC Adv.* 7, 22706–22714. <https://doi.org/10.1039/C7RA01060E>  
16 716 Zhang, D., Cai, C., Zhu, J., 2021. Changes of Soil Water–Stable Aggregates after Rice–Crawfish Rotation in  
17 717 Low-lying Paddy Fields: A Case Study in Jiangnan Plain of China. *Commun. Soil Sci. Plant Anal.* 52,  
18 718 2358–2372. <https://doi.org/10.1080/00103624.2021.1928169>  
19 719 Zhu, J.Y., Sabo, R., Luo, X., 2011. Integrated production of nano-fibrillated cellulose and cellulosic biofuel  
20 720 (ethanol) by enzymatic fractionation of wood fibers. *Green Chem.* 13, 1339–1344.  
21 721 <https://doi.org/10.1039/C1GC15103G>  
22 722  
23  
24  
25  
26  
27  
28  
29  
30  
31  
32  
33  
34  
35  
36  
37  
38  
39  
40  
41  
42  
43  
44  
45  
46  
47  
48  
49  
50  
51  
52  
53  
54  
55  
56  
57  
58  
59  
60  
61  
62  
63  
64  
65

# A nature-based approach to enhance the potential application of forest residues in anaerobic digestion

**Abstract:** Forest residues and other woody wastes are abundant and require management. Anaerobic digestion (AD) is a potential disposal option for such waste, but the absence of cost-effective pretreatment technologies hinders their utilization in AD. This paper presents a nature-based approach for improving AD performance of forest residues, relying on the lignocellulose degradation processes inherent in the forest ecosystem. Wood samples at five decay classes (numbered 1-5 with increasing decay) were collected for series of experiments. Physicochemical analysis showed that higher decay class samples presented a series of characteristics favourable to AD. Wood samples from decay class 1 had the lowest methane yield, while decay class 3 had the highest, with a notable 160% increase compared to decay class 1. The outcomes identify the stage of highest methane production from forest residues, allowing for strategic collection to improve the economic viability of using forest residues as feedstock for AD applications.

**Keywords:** Forest residues; Woody waste; Anaerobic digestion; Methane production; Pretreatment technology; Forest soil ecosystem

## Nomenclature

AD: anaerobic digestion; DC: decay class; VS: volatile solids; SEC: specific energy consumption; MWD: mean weight diameter; FD: fractal dimension; TS: total solids; TOC: total organic carbon; WEOC: water extractable organic carbon; CrI: cellulose crystallinity index; ORP: oxidation reduction potential; TMP: theoretical methane production; BD: anaerobic biodegradability; EMP: experimental methane production; PMP: predicted methane production.

## 1 Introduction

The anaerobic digestion (AD) of renewable biomass, including woody biomass, is emerging as a sustainable energy source due to its availability, low cost, and minimal environmental impact (Gao et al., 2025; Manikandan et al., 2023). Recent studies highlight that pretreatment techniques significantly enhance methane production from woody biomass, underscoring its potential as a AD feedstock (Gao et al., 2024a). A variety of pretreatment approaches have been developed to breakdown the recalcitrant structure of woody biomass, including biological, chemical, and physical processes (Gao et al., 2022; Hashemi et al., 2022). While physical methods require large energy inputs and high equipment cost for the specific conditions (Atelge et al., 2020; Gao et al., 2024b), and chemical methods risk environmental contamination (Dai et al., 2018; Tian et al., 2016), biological methods show potential despite challenges in isolating effective microorganisms and the lengthy, labor-intensive process (Alexandropoulou et al., 2017; Ali et al., 2017). In view of this, it is important to consider and develop alternative technologies for the pretreatment of woody biomass to boost methane production in a more sustainable way.

1 43 In forest ecosystems, dead trees play a crucial ecological role by decomposing and  
2  
3  
4 44 releasing stored nutrients (Seibold et al., 2021). The decomposition process, involving fungi,  
5  
6 45 bacteria, and arthropods, spans several years and creates a complex community (Tarasov et  
7  
8  
9 46 al., 2018; Yoon et al., 2023). Due to the complexity of the natural wood degradation process  
10  
11  
12 47 in forest ecosystems, it is difficult to simulate and apply this system as a pretreatment method  
13  
14  
15 48 for woody biomass under experimental conditions. Notably, large quantities of forest  
16  
17  
18 49 residues are generated during timber harvesting and from forest maintenance treatments such  
19  
20  
21 50 as cleaning and thinning (Pergola et al., 2022). It is estimated that there are approximately  
22  
23  
24 51 230,000 hectares of plantation forests in Queensland, with up to 600,000 tons of forest  
25  
26  
27 52 residues generated by logging annually (Garvie et al., 2021). Kurvits et al. (2020)  
28  
29  
30 53 investigated the quantity of logging residues at four forest sites in Southeast Estonia from  
31  
32  
33 54 2013 to 2014 and found that forest residues reached up to a dry weight of 29 tons per hectare.  
34  
35  
36 55 Unless harvested for application, the fate of these forest residues is to be degraded into humus  
37  
38  
39 56 as part of the forest soil. During this degradation process, the texture of the wood will  
40  
41  
42 57 gradually become soft, as the rigid and recalcitrant lignocellulosic structure is slowly  
43  
44  
45 58 destroyed, with the wood finally being completely decomposed to release all the nutrients  
46  
47  
48 59 (Petritan et al., 2023; Shorohova et al., 2021).

49 60 An interesting aspect of this natural degradation process is that it tends to predispose  
50  
51  
52 61 wood waste for AD applications due to the increased accessibility and biodegradability of  
53  
54  
55 62 the lignocellulosic structure. In addition, the softened texture of the material allows them to  
56  
57  
58 63 be shredded more easily, which can also save the energy required to pre-process the material  
59  
60  
61 64 prior to AD. We hypothesize that exposing woody wastes to forest ecosystems for a period  
62  
63  
64  
65

1 65 of time is sufficient to enhance its digestibility as part of a pretreatment process prior to AD.  
2  
3  
4 66 In addition, the collection and valorisation of such residues can help to mitigate forest  
5  
6 67 management costs, reducing fire risk and additional emissions from degradation (Lee and  
7  
8  
9 68 Han, 2017; Molenda et al., 2021; Nicholls et al., 2018). The objectives of this study were to  
10  
11  
12 69 determine the differences in physicochemical composition and the methane production  
13  
14  
15 70 potential between wood samples at different stages of decay from forest environments.  
16  
17  
18 71 Identifying the decay stage at which the wood waste can have the highest methane production  
19  
20  
21 72 allows for strategic collection of this material, enhancing the economic viability of using  
22  
23  
24 73 wood waste as a raw material in AD applications.

## 27 74 **2 Materials and methods**

### 30 75 **2.1 Experimental materials**

33 76 The wood samples were collected from two sites, with Site 1 being an unmanaged  
34  
35  
36 77 seminatural forest in Cardiff, UK (51°31'4"N, 3°14'46"W) and Site 2 being a large managed  
37  
38  
39 78 forest in Cardiff, UK (51°32'25"N, 3°14'58"W). At each site, at least 15 dead fallen logs were  
40  
41  
42 79 sampled, each of which was allocated to a particular *decay class* (DC), determined based on  
43  
44  
45 80 visual and mechanical inspections (Table S1), with DC1 showing minimal signs of decay and  
46  
47  
48 81 DC5 showing highly advanced levels of decay (Tatti et al., 2018). Considering the external  
49  
50  
51 82 appearance and the species of the surrounding trees, the wood samples from Site 1 were  
52  
53  
54 83 probably hardwood silver birch (*Betula pendula*), expressed here as Birch. The sampling  
55  
56  
57 84 location at Site 2 consists primarily of European ash (*Fraxinus excelsior*), expressed in this  
58  
59  
60 85 paper as Ash, confirmed from site records and by examining the surrounding tree morphology.  
61  
62  
63  
64  
65

1 86 Wood samples were dried and then shredded using a Fritsch 55743 rotary knife mill with a 2  
2  
3  
4 87 mm screen and finally stored at 4 °C until further analysis.  
5  
6

## 7 88 2.2 Experimental procedure

8  
9  
10 89 The AD experimental apparatus, consisting of multiple 1L bioreactors in a temperature-  
11  
12  
13 90 controlled water bath with gas collection facility, was supplied by Anaero Technology UK,  
14  
15  
16 91 described in more detail by Muaaz-Us-Salam et al. (2020). Sewage sludge digestate from an  
17  
18  
19 92 AD reactor was used as an anaerobic inoculum. Prior to AD testing, the sludge was incubated  
20  
21  
22 93 at 35 °C for 3 days and shaken manually twice a day to ensure homogenization. For every  
23  
24  
25 94 experiment, fresh sludge was sampled from the same AD reactor. Each bioreactor was filled  
26  
27  
28 95 with 700 mL of inoculum with a headspace volume of 300 mL. Then a certain mass of wood  
29  
30  
31 96 samples at different DC was added, the blank group did not have any wood sample added  
32  
33  
34 97 (only 700 mL inoculum). The weight of wood samples in each reactor was calculated to  
35  
36  
37 98 ensure the ratio of decaying wood samples to inoculum was 1:4 based on volatile solids (VS)  
38  
39  
40 99 levels. All bioreactors were incubated at 35 °C for 35 days with continuous stirring at 45 rpm.  
41  
42 100 Liquid samples (5 mL) were taken during the AD process using sterile pipettes and  
43  
44  
45 101 transferred to 15 mL sterile containers for the measurement of some parameters during the  
46  
47  
48 102 AD process. Biogas produced from each reactor was collected during the experiment in 5 L  
49  
50  
51 103 Tedlar gas bags and analyzed for methane content (see section 2.3.4). The AD experiments  
52  
53  
54 104 were performed in triplicate for each wood sample and in duplicate for the blank group (only  
55  
56  
57 105 inoculum).  
58

## 59 106 2.3 Analytical methods

### 2.3.1 Specific energy consumption for grinding

The effect of DC on specific energy consumption (SEC) during shredding (comminution) was determined. A Fritsch 55743 rotary knife mill was used, equipped with a 2 mm screen and a 2100 W motor. For all samples, a pre-weighed 50 grams wood block (dry matter) was placed in the rotary knife mill for 60 seconds, and then the wood collected in the tray was weighed. The SEC was calculated according to Equation (1) as presented in previous literature (Miao et al., 2011; Moiceanu et al., 2019).

$$\text{SEC} = \frac{P \times T}{m} \quad (1)$$

where SEC is total specific energy consumption for grinding a unit of dry matter (MJ/kg of dry matter);  $P$  is the power of the milling machine while grinding wood samples;  $T$  is the total time of grinding operations;  $m$  is dry matter mass (kg) of wood samples collected in the tray.

### 2.3.2 Analysis of particle size distribution

Particle size distribution was measured using sieving methods. Specifically, wood samples were put into a Fritsch 55743 rotary knife mill equipped with a 2 mm screen and operated for 1 min. The collected sample was passed through a tower of differently sized sieves. The sieve stack contained stainless steel sieves (diameter 200 mm) with mesh sizes of 2000, 1000, 500, 250, 125, and 75  $\mu\text{m}$ . The sieving steps were performed on a vibratory shaker (Matest A060-01) for 30 min to ensure adequate separation of the samples. Samples were finally sieved into seven fractions (<75, 75–125, 125–250, 250–500, 500–1000, 1000–2000, and >2000  $\mu\text{m}$ ), and the proportion of samples in each particle size class was calculated based on the weight.

1 128 The mean weight diameter (MWD) and fractal dimension (FD) can be applied to further  
2  
3  
4 129 characterize the particle size of the sample (Rabot et al., 2018; Zhang et al., 2021). MWD is  
5  
6 130 the sum of the weighted mean diameters of all size classes, whilst FD is a comprehensive  
7  
8  
9 131 indicator of sample composition and textural homogeneity. The MWD of dry-sieved samples  
10  
11  
12 132 was calculated using Equation (2):

$$\text{MWD} = \sum_{i=1}^n \frac{r_i + r_{i+1}}{2} \times m_i \quad (2)$$

13 133 where  $r_i$  is the aperture of the  $i$ th sieve,  $m_i$  is the proportion of sample weight remaining on  
14  
15  
16  
17  
18  
19  
20  
21  
22 134 the  $i$ th sieve, and  $n$  is the number of sieves. The FD was calculated using Equation (3):

$$\frac{M(r < R_i)}{M_r} = \left(\frac{R_i}{R_{max}}\right)^{3-FD} \quad (3)$$

23  
24  
25  
26  
27  
28 135 where  $M(r < R_i)$  is the cumulative sample mass with a radius smaller than  $R_i$ ,  $M_r$  is the total  
29  
30  
31  
32 136 sample mass with a radius smaller than  $R_{max}$ ,  $R_i$  is the radius of each dimensional fraction,  
33  
34 137  $R_{max}$  is the maximum radius, and FD is the fractal dimension of the sample.

### 35 36 37 138 2.3.3 Physicochemical features of solid samples

38  
39  
40 139 Total solids (TS) and VS of the wood samples were measured following the Standard  
41  
42  
43 140 Methods 2540 protocol (Rice et al., 2017). The ultimate analysis (carbon, hydrogen, nitrogen,  
44  
45  
46 141 and oxygen content) was measured using an elemental analyzer (Flash Smart, Thermo Fisher  
47  
48  
49 142 Scientific Co., USA). Cellulose, hemicellulose, and lignin contents were determined by  
50  
51  
52 143 thermogravimetric analysis (Díez et al., 2020; Rego et al., 2019), and the detailed approach  
53  
54 144 is shown in the Supporting Information (Text S2). The total organic carbon (TOC) of wood  
55  
56  
57 145 samples were measured with a TOC-VCPH (Shimadzu, Kyoto, Japan) following the  
58  
59  
60 146 manufacturer's instructions. The analysis of water extractable organic carbon (WEOC) was

1 147 modified from Mo et al., (2022). Specifically, a total of 5 g of shredded wood was added to  
2  
3  
4 148 30 mL of Milli-Q water and shaken at 200 rpm for 2 h at room temperature. The supernatant  
5  
6 149 was subsequently filtered through sterile 0.45 µm filters and stored in the dark at 4 °C prior  
7  
8  
9 150 to further analyses. Finally, the WEOC concentrations were measured by a TOC-VCPH  
10  
11  
12 151 (Shimadzu, Kyoto, Japan) following the manufacturer's instructions.  
13  
14

15 152 The crystallinities of all decaying wood samples were measured using a X'Pert<sup>3</sup> MRD  
16  
17  
18 153 XL Materials Research X-ray Diffraction System (Malvern Panalytical, Malvern, UK)  
19  
20  
21 154 equipped with with CuK $\alpha$  radiation. Scans were obtained from  $2\theta = 10\text{--}40^\circ$  with step size of  
22  
23  
24 155 0.02 at 0.6 s per step. The cellulose crystallinity index (CrI) of the samples can be calculated  
25  
26  
27 156 according to Equation (4):

$$\text{CrI} = \frac{I_{002} - I_{am}}{I_{002}} \times 100 \quad (4)$$

28  
29  
30  
31  
32  
33 157 where  $I_{002}$  is intensity of diffraction from 002 plane at  $2\theta = 22^\circ$  and  $I_{am}$  is the intensity of  
34  
35  
36 158 background measured at  $2\theta = 18^\circ$  (Kumar et al., 2019; Liu et al., 2015).  
37  
38

#### 39 159 2.3.4 Physicochemical features of liquid and gas samples 40 41

42 160 TS and VS of the inoculum were measured following the standard methods (Rice et al.,  
43  
44  
45 161 2017). The inoculum was dried and subjected to ultimate analysis with an elemental analyzer  
46  
47  
48 162 (Flash Smart, Thermo Fisher Scientific Co., USA). The pH and oxidation reduction potential  
49  
50  
51 163 (ORP) of inoculum and liquids samples collected during AD experiments were measured by  
52  
53  
54 164 a freshly calibrated pH probe (Mettler-Toledo, Switzerland) and a freshly calibrated ORP  
55  
56  
57 165 probe with an Ag/AgCl electrode (Mettler-Toledo, Switzerland). All 5 mL liquid samples  
58  
59 166 obtained during AD experiments were filtered through sterile 0.45 µm filters. Subsequently,  
60  
61  
62  
63  
64  
65

1 167 a 2 mL filtered sample was added to 18 mL Milli-Q water (10 times dilution) and mixed  
2  
3  
4 168 thoroughly for TOC measurement.  
5

6 169 The biogas production in each bioreactor was determined by gas flow meters  
7  
8  
9 170 incorporated within the AD apparatus combined with data logging equipment, and the  
10  
11  
12 171 methane content of the biogas was determined using a portable biogas analyzer (RASI 700  
13  
14  
15 172 BIO, Eurotron Instruments UK ltd, Germany). The instrument was calibrated using a series  
16  
17  
18 173 of standard gases with concentration gradients (labeled methane concentration) prior to  
19  
20  
21 174 testing the methane content in the samples.  
22

### 23 175 2.3.5 Calculation and prediction of methane production

24  
25  
26 176 The theoretical methane production (TMP) of wood samples was calculated from the  
27  
28  
29 177 elemental composition (expressed in molar fractions) using the Buswell formulae (Lübken et  
30  
31  
32 178 al., 2010), Equations (5) and (6):  
33

$$34 \quad C_n H_a O_b N_c + \left( n - \frac{a}{4} - \frac{b}{2} + \frac{3c}{4} \right) H_2O$$
$$35 \quad \rightarrow \left( \frac{n}{2} + \frac{a}{8} - \frac{b}{4} - \frac{3c}{8} \right) CH_4 + \left( \frac{n}{2} - \frac{a}{8} + \frac{b}{4} + \frac{3c}{8} \right) CO_2 + cNH_3$$

36  
37  
38  
39  
40  
41

$$42 \quad TMP = 22.4 \times \left( \frac{n}{2} + \frac{a}{8} - \frac{b}{4} - \frac{3c}{8} \right) / (12n + a + 16b + 14c)$$

43  
44  
45

46 179 The anaerobic biodegradability (BD) of wood samples was calculated according to  
47  
48  
49 180 Equation (7):  
50

$$51 \quad BD (\%) = \text{Experimental methane production (EMP)} / TMP \times 100$$

52  
53  
54

55 181 The experimental biogas production was fitted using a modified Gompertz kinetic model,  
56  
57 182 which is one of the most commonly employed models in the literature for fitting biogas  
58  
59  
60 183 production (Isha et al., 2021). The final biogas production was calculated based on the best-  
61  
62

1 184 fit Gompertz model and then multiplied by the methane content to obtain the predicted  
2  
3  
4 185 methane production (PMP). The kinetic model is shown in Equation (8):

$$M = P_b \times \exp \left\{ -\exp \left[ \frac{R_m \times e}{P_b} (\lambda - t) + 1 \right] \right\} \quad (8)$$

5  
6  
7  
8  
9  
10 186 where  $M$  is the biogas production (mL/g of VS) relative to the time  $t$  (d);  $P_b$  is the maximum  
11  
12  
13 187 biogas potential of the substrate (mL/g of VS);  $R_m$  is the maximum biogas production rate  
14  
15  
16 188 (mL/g of VS.d),  $\lambda$  is the lag phase time taken for biogas production (1/d),  $e$  is Euler's number  
17  
18  
19 189 which is taken here as 2.7183.

20  
21  
22 190 Furthermore, there was no well-developed model available to predict the methane  
23  
24  
25 191 production from AD of wood waste. Our previous study generated a machine learning model  
26  
27  
28 192 with good predictive performance, which was applied in this study to predict methane  
29  
30  
31 193 production from all decayed wood samples (Gao et al., 2024a). In the previous publication,  
32  
33  
34 194 1179 groups of datasets were collected for the machine learning analysis, which included  
35  
36  
37 195 nine input variables, namely wood types, inoculum types, volume (mL), temperature (°C),  
38  
39  
40 196 particle size (mm), ratio of inoculum to substrate (based on VS), cellulose content (%),  
41  
42  
43 197 hemicellulose content (%), lignin content (%), and digestion time (d), where wood types and  
44  
45  
46 198 inoculum types were represented as categorical objects. The random forest machine learning  
47  
48  
49 199 method was found to have the highest prediction accuracy and was used in this study.

## 50 51 200 2.4 Statistical analysis

52  
53  
54 201 In this paper, statistical analyses were done using Origin 2021. All values are presented  
55  
56  
57 202 as the mean  $\pm$  s.d., unless otherwise specified. Statistical significance was assessed using the  
58  
59  
60 203 two-tailed Student's t-test or One-way ANOVA test with significance at a  $p$  value of 0.05.

1 204 Moreover, The Pearson correlation coefficients ( $r$ ) between the variables were also calculated.

2  
3 205 The strength of the correlation was described by the absolute value of  $r$  (0.00–0.19 very weak;

4  
5  
6 206 0.20–0.39 weak; 0.40–0.59 moderate; 0.60–0.79 strong; 0.80–1.0 very strong).

## 7 8 9 207 **3 Results and discussion**

### 10 11 12 208 **3.1 Energy consumption and particle size analysis**

13  
14  
15  
16 209 Generally, mechanical pretreatment is considered as the most important and promising  
17  
18 210 preliminary step for handling and converting biomass into bioenergy before proceeding to  
19  
20  
21 211 the next process (Kamarludin et al., 2014). Without a sufficiently small particle size or large  
22  
23  
24 212 relative surface area, the organic matter in the substrate cannot be utilized by microorganisms  
25  
26  
27 213 to produce biogas during AD. For example, 2 cm wood cubes in digested sewage sludge  
28  
29  
30 214 produced approximately the same amount of biogas as blanks with only sludge (Gao et al.,  
31  
32  
33 215 2023; Muaaz-Us-Salam et al., 2020). As shown in Fig. 1, the SEC gradually decreased as DC  
34  
35  
36 216 increased. Fig. 1a shows that the SEC of Birch decreased from 10.56 to 2.92 MJ/kg of dry  
37  
38  
39 217 matter for DC1 to DC5, while Ash correspondingly dropped from 9.44 to 2.60 MJ/kg of dry  
40  
41  
42 218 matter (Fig. 1b). In addition, the decrease rate of SEC for both wood samples gradually  
43  
44  
45 219 became slower with increased DC, showing no statistical difference between wood samples  
46  
47  
48 220 from DC3 to DC5. These results imply that the higher the DC, the more energy can be saved  
49  
50  
51 221 in reducing the particle size of these wood samples for utilization in AD. It is worth noting  
52  
53  
54 222 that the criteria for these DC include their hardness, with DC5 being extremely soft due to its  
55  
56  
57 223 woody structure has been essentially destroyed (Tatti et al., 2018). During the sampling, it  
58  
59  
60  
61  
62  
63  
64  
65

1 224 was found that DC4 and DC5 can be broken even with slight force by hand. Therefore, wood  
2  
3  
4 225 samples with high DC may not require physical pre-processing.  
5

6 226 Reducing the particle size of substrates is a competitive option for increasing methane  
7  
8  
9 227 production from AD as it releases more organic matter and cell compounds, and directly  
10  
11  
12 228 increases the microbially accessible surface area, thus improving biodegradability (Dai et al.,  
13  
14  
15 229 2019). After grinding the samples, we analyzed their particle size distribution (Table 1). The  
16  
17  
18 230 samples of DC1 and DC2 had the highest proportion in the 1–2 mm particle size class, and  
19  
20  
21 231 the proportion decreased as the particle size class increased. The proportion of the fine  
22  
23  
24 232 particle size class gradually increased from DC1 to DC5, with the proportion of 0.5–1 mm  
25  
26  
27 233 particle size class being the largest in DC4 and DC5. In addition, the MWD analysis also  
28  
29  
30 234 showed the particle size of wood samples reduced gradually from DC1 to DC5. Specifically,  
31  
32  
33 235 the MWD of Birch decreased from 0.93 to 0.57 mm for DC1 to DC5, while Ash  
34  
35  
36 236 correspondingly dropped from 1.10 to 0.78 mm (Table 1). Reduced particle size can  
37  
38  
39 237 significantly facilitate hydrolysis and acidification processes, resulting in increased volatile  
40  
41  
42 238 fatty acid content and VS degradation (Luo et al., 2021). Liu et al. (2017) reported the effects  
43  
44  
45 239 of particle size of two forest residues on methane production through AD batch experiments,  
46  
47  
48 240 and the results showed that methane yield improved when the substrate particle size was  
49  
50  
51 241 reduced from 4 mm to 1 mm. A similar pattern has been demonstrated in other lignocellulosic  
52  
53  
54 242 wastes, such as rice straw, where methane production improved with a decrease in substrate  
55  
56  
57 243 particle size (Dai et al., 2019; Ji et al., 2022).

58 244 Fractal theory has been applied to quantitatively assess the basic morphology of the  
59  
60  
61 245 substrate, which is a potential indicator reflecting the AD efficiency (Wang et al., 2016). In  
62  
63  
64  
65

1 246 this study, the FD of different DC samples were statistically different ( $p<0.05$ ) after grinding  
2  
3  
4 247 under the same conditions. As shown in Table 21, the FD average of both wood samples at  
5  
6 248 DC1 was significantly lower than DC5 ( $p<0.05$ ), while there were no significant differences  
7  
8  
9 249 in FD values between DC3, DC4 and DC5 ( $p>0.05$ ). The increase in FD can enhance the  
10  
11  
12 250 particle translational velocities in the horizontal direction while decreasing the rotational  
13  
14  
15 251 velocity, and the amount of particles participated in horizontal dispersion increased due to  
16  
17  
18 252 the reduction in the intensity of the contact shear particle behavior, which effectively  
19  
20  
21 253 promoted particle diffusion (Lai et al., 2021). Therefore, the DC5 samples may have  
22  
23  
24 254 enhanced mobility in the AD system compared to the DC1 samples, which facilitates its full  
25  
26  
27 255 utilization by microbes. Moreover, the wood samples after DC3 showed no significant  
28  
29  
30 256 difference, suggesting that this class (DC3) may achieve optimal conditions for sample  
31  
32 257 crushing.

### 36 258 3.2 Physicochemical features analysis of decaying wood samples

39 259 The possibility of using these wood samples as a suitable substrate for AD was primarily  
40  
41  
42 260 verified through various tests, prior to conducting the biomethane potential experiments. As  
43  
44  
45 261 shown in Table 2, TS content decreased with DC, while the VS content did not change much.  
46  
47  
48 262 Samples with a high DC have a looser texture, which allows them to easily retain more water.  
49  
50  
51 263 Compared to Ash, in general Birch had a smaller TS content and a much larger drop from  
52  
53  
54 264 DC1 (59.47%) to DC5 (18.39%). For lignocellulosic biomass, the nitrogen content is a key  
55  
56  
57 265 factor limiting their AD performance (Song et al., 2024). A low level of nitrogen can lead to  
58  
59  
60 266 nitrogen limitation, which prevents the microorganisms from fully utilizing the carbon source,

1 267 thus reducing the production of methane (Piątek et al., 2016). The total carbon in all five DC  
2  
3  
4 268 were nearly the same, but the nitrogen content was higher in the high DC samples. Therefore,  
5  
6 269 the carbon to nitrogen ratio of DC5 was much lower than that of DC1. It has been reported  
7  
8  
9 270 that the optimal carbon to nitrogen ratio for maximal methane production is between 20 and  
10  
11  
12 271 30 (Kumar et al., 2021). Although the carbon to nitrogen ratio of DC5 samples was also  
13  
14  
15 272 higher than the optimal value, it is easier to achieve the superior system by mixing them with  
16  
17  
18 273 sludge (low carbon to nitrogen ratio). During AD, TOC can be biodegraded in hydrolysis,  
19  
20  
21 274 acidification and methanation steps to produce biogas (Provenzano et al., 2014). Furthermore,  
22  
23  
24 275 WEOC is a critical contributor in these processes, as microbial metabolism occurs in the  
25  
26  
27 276 water-soluble phase (Xing et al., 2012). Therefore, the significantly higher TOC (Fig. 2a and  
28  
29  
30 277 2b) and WEOC (Fig. 2c and 2d) in high DC samples indicate a better potential for methane  
31  
32  
33 278 production from AD. It is noteworthy that the WEOC did not consistently increase with decay  
34  
35  
36 279 level, showing a tendency of first increasing and then decreasing. The DC3 samples of Birch  
37  
38  
39 280 had the highest WEOC (Fig. 2c), and the DC4 samples of Ash had the highest WEOC (Fig.  
40  
41  
42 281 2d). This might be due to the release of organic matter from the forest residues in the presence  
43  
44  
45 282 of insects and microorganisms, leading to an increase in WEOC content at the beginning of  
46  
47  
48 283 decay process. When it reaches the final stages of decomposition, there is no more organic  
49  
50  
51 284 matter to be released, and the previously released organic matter is utilized by other  
52  
53  
54 285 organisms or enters the soil, leading to a decrease in the WEOC content.

55 286 The lignocellulose composition is an important factor that affects the AD performance  
56  
57  
58 287 of forest residues. Fig. S1 and S2 show the thermogravimetric experimental data and  
59  
60  
61 288 derivative thermogravimetric curves fitting results using the Gaussian model, and the

1 289 calculated lignocellulose composition of all wood samples are provided in Table 2. In both  
2  
3  
4 290 types of wood samples, the cellulose content decreased with DC, in contrast with a gradually  
5  
6 291 increased lignin content. The hemicellulose content did not vary much among the five DC  
7  
8  
9 292 samples, and two types of wood samples showed different tendencies. With an increase in  
10  
11  
12 293 DC, Birch presented an overall decrease, while Ash first decreased and then increased. The  
13  
14  
15 294 significantly increased lignin content of higher DC may be due to the reduction of other  
16  
17  
18 295 components such as cellulose, indicating that the forest soil system was not effective in  
19  
20  
21 296 removing lignin of forest residues, and it became proportionally more significant as a  
22  
23  
24 297 component as decay occurred. However, the decay has permitted biological access to, and  
25  
26  
27 298 degradation of, cellulose and hemicellulose, suggesting that a certain amount of decay and  
28  
29  
30 299 breakdown may be advantageous as a pretreatment method for AD. Similar effects have been  
31  
32  
33 300 observed in other studies, such as the application of chemicals (Mohsenzadeh et al., 2012;  
34  
35 301 Salehian et al., 2013), hydrothermal (Karami et al., 2022) and steam explosion (Eom et al.,  
36  
37  
38 302 2019; Mulat et al., 2018) leading to a reduction in the cellulose content and an increase in the  
39  
40  
41 303 lignin content of wood waste.

42  
43  
44 304 Due to the presence of crystalline cellulose in biomass samples, the  $2\theta$  value of X-ray  
45  
46  
47 305 diffraction shows a sharp peak between  $18^\circ$  and  $22^\circ$  (Awoyale and Lokhat, 2021). Cellulose  
48  
49  
50 306 crystallinity reflects the proportion of cellulose crystalline regions, and the CrI of the  
51  
52  
53 307 substrate determines its biodegradability during AD. The CrI of Birch DC1 samples was  
54  
55 308 35.43%, close to the value of raw pine wood; and the CrI of Ash DC1 samples (41.61%) was  
56  
57  
58 309 close to that of untreated acacias (Darmawan et al., 2016). It indicated that the degradation  
59  
60  
61 310 of DC1 samples was quite small, and its CR nearly approached that of fresh wood. The CrI

1 311 of DC5 samples was much lower than that of DC1 samples, with a value of 16.47% in Birch  
2  
3  
4 312 and 26.43% in Ash (Fig. 3). As mentioned above, this may be due to the different composition  
5  
6 313 in different DC samples. The content of soluble matter and amorphous cellulose in  
7  
8  
9 314 lignocellulosic biomass is higher than that of crystalline cellulose, which can result in a lower  
10  
11  
12 315 CrI (D' Silva et al., 2022). The hydrolysis of amorphous cellulose by cellulase was found to  
13  
14  
15 316 be about 30 times faster than that of crystalline cellulose (Zhu et al., 2011). The low CrI value  
16  
17  
18 317 in DC5 samples meant that their cellulose crystalline region was destroyed, leaving more  
19  
20  
21 318 cellulose (amorphous cellulose) available for microbial hydrolysis. Moreover, it was found  
22  
23  
24 319 that corn straw pretreatment with hydrogen-nanobubble water (He et al., 2022) or a pure  
25  
26  
27 320 bacteria system (Xu et al., 2018) also reduced the CrI of substrate and enhanced the methane  
28  
29  
30 321 production from AD of corn straw. Therefore, the forest soil system could degrade the  
31  
32  
33 322 cellulose crystallinity, allowing the forest residues to decompose more easily by AD.

### 34 35 36 323 3.3 Effect of five decay classes on anaerobic digestion performance

37  
38  
39 324 The patterns of daily biogas yield were shown in Fig. 4a and 4b. As higher DC samples  
40  
41  
42 325 had lower MWD (Table 1), resulting in a larger surface area, they would be more susceptible  
43  
44  
45 326 to hydrolysis and acidification compared to DC1 samples, producing more feedstock for  
46  
47  
48 327 methanogen utilization. To further explore the effects of particle size on biogas production,  
49  
50  
51 328 the Birch DC1 and DC3 samples with same particle size were selected for a separate AD  
52  
53  
54 329 experiment. Although the biogas yield of Birch DC3 samples was still considerably higher  
55  
56  
57 330 than that of DC1 samples, the gap between these samples at the same particle size was smaller  
58  
59  
60 331 than the previous (Fig. S3). It was also noted that all DC samples showed high daily biogas  
61  
62  
63  
64  
65

1 332 yield in the initial few days. During the early stages of AD, the feedstock is mainly  
2  
3  
4 333 hydrolyzed and acidified, and the primary contributors to the biogas are WEOC from the  
5  
6 334 wood samples and the residual organic matter in the sludge.  
7  
8

9 335 As shown in Fig. 4c and 4d, the net cumulative biogas yield varied significantly among  
10  
11  
12 336 different DC samples. These curves showed a rapid increase in biogas within the first 10 days,  
13  
14  
15 337 reaching about 50% of the total output. The final biogas yield increased from DC1 to DC3  
16  
17  
18 338 (Birch) and DC3/4 (Ash) before decreasing at higher DC. For Birch, the biogas yield of DC3  
19  
20  
21 339 samples was 3.52 times higher than that of DC1 samples, but this value narrowed down to  
22  
23  
24 340 2.14 at the same particle size (Fig. S3). This result suggested that decayed wood, besides  
25  
26  
27 341 increasing biogas production by being more prone to small particle sizes, had  
28  
29  
30 342 physicochemical properties that were more favorable for microbial utilization in AD system.  
31  
32 343 Fig. S4 illustrates the effect of DC on pH, ORP and TOC during AD. The initial phase of AD,  
33  
34  
35 344 which mainly involves the process of substrate hydrolysis and acidification, leads to a  
36  
37  
38 345 continuous accumulation of volatile fatty acids (He et al., 2022). The results showed that the  
39  
40  
41 346 pH decreased continuously after the AD started and reached the lowest value on the 5th day.  
42  
43  
44 347 The redox potential of the AD system can affect the microbial growth activities, and low  
45  
46  
47 348 redox potential means more strict anaerobic conditions and stronger reduction (Xu et al.,  
48  
49  
50 349 2014). Methane production requires the consumption of reducible substances. The  
51  
52  
53 350 breakdown of organic matter caused an initial increase in TOC content of the liquid phase,  
54  
55  
56 351 which then declined as methanogens utilized these materials to produce methane. The  
57  
58  
59 352 Pearson correlation analyses also revealed that these parameters were correlated with biogas  
60  
61 353 yields (Fig. S5).  
62  
63  
64  
65

1 354 Although the biogas production differed considerably between different DC, the  
2  
3  
4 355 methane content of these biogas did not vary greatly, with an overall value of around 60%  
5  
6 356 (Fig. 5). According to the final measurements, the highest values of net methane yield were  
7  
8  
9 357 found in the DC3 or DC4 samples after 35 d, with 134.76 and 142.51 mL/g VS for the Birch  
10  
11  
12 358 DC3 and Ash DC4 samples, respectively. The theoretical methane production, calculated by  
13  
14  
15 359 the elemental composition using the Buswell formula, did not differ significantly between  
16  
17  
18 360 different DC (Table S3). Therefore, the biodegradability index corresponded to the total  
19  
20  
21 361 biogas yield results, with DC3 samples being the highest and DC1 samples the lowest. The  
22  
23  
24 362 degradation of wood in the forest did not significantly change its elemental (carbon, hydrogen,  
25  
26  
27 363 oxygen, and nitrogen) composition (Table 2). However, due to the extremely low content of  
28  
29  
30 364 nitrogen in fresh wood, a slight increase in nitrogen can significantly shift the carbon to  
31  
32  
33 365 nitrogen ratio, making the samples more applicable to AD.

### 366 3.4 The fitting and prediction of methane yield

39 367 To investigate the methanogenic kinetics, a modified Gompertz model was employed to  
40  
41  
42 368 fit the cumulative biogas yield curves, and the kinetic parameters of fitting results are shown  
43  
44  
45 369 in Table S4. The lag period is a parameter that reflects the adaptation of microbes to the AD  
46  
47  
48 370 system during the initial stage (Mao et al., 2017). As shown in Table S4, the DC3 digesters  
49  
50  
51 371 had the shortest lag period, which is attributed to these samples having the highest WEOC  
52  
53  
54 372 content, being rapidly hydrolyzed and converted to methane. It can be seen that the maximum  
55  
56  
57 373 biogas potential corresponds quite well to the experimental values. In addition, the maximum  
58  
59  
60 374 specific biogas production rate of digester DC3 and DC4 samples were noticeably higher

1 375 than that of other digesters, which was in good agreement with the experimental results.

2  
3 376 Overall, all cumulative biogas yield curves can be well fitted by the modified Gompertz

4  
5  
6 377 model, and the correlation coefficient of fitting results was between 0.95 and 0.99.

7  
8  
9 378 Prior to performing AD, it is desirable to determine the optimal parameters for maximum

10  
11  
12 379 methane yield from woody waste. To the best of our knowledge, an approach that can predict

13  
14  
15 380 methane yield from woody waste while addressing the issues involved in identifying the

16  
17  
18 381 optimal digestion conditions and feedstock properties to maximize methane yield has not yet

19  
20  
21 382 been developed. As shown in Table S3, the random forest model predicted biogas production

22  
23  
24 383 well with an error rate of around 25%. The machine learning model (random forest)

25  
26  
27 384 prediction accuracies of some samples were close to the results of the Gompertz fitting,

28  
29  
30 385 indicating that the machine learning model is instructive in practical AD with woody waste.

31  
32  
33 386 It is worth noting that the predictions for the Birch DC1 samples were less accurate. This

34  
35  
36 387 may be because the previously established database for creating machine learning models

37  
38  
39 388 was not comprehensive and lacked data on this part of relatively low methane production

40  
41  
42 389 (Gao et al., 2024a). Therefore, more experiments on AD of woody biomass are needed in the

43  
44 390 future in order to expand the database for improving the model.

### 45 46 47 391 3.5 Applications and Future considerations

48  
49  
50 392 The present study introduces a novel nature-based approach to enhance suitability of

51  
52  
53 393 wood waste, particularly forest residues, for AD, providing a sustainable solution to two key

54  
55  
56 394 issues that have hampered the practical application of wood waste AD. Firstly, the low

57  
58  
59 395 methane production from wood has been overcome with an average increase of 160% in

1 396 methane yield after this nature-based approach (DC3 compared to DC1). This is comparable  
2  
3  
4 397 to other, more intensive, pretreatment technologies such as combined  
5  
6 398 hydrothermal/enzymatic treatment (168% improvement) (Matsakas et al., 2015), aqueous  
7  
8  
9 399 ammonia soaking (151% improvement) (Antonopoulou et al., 2015), or combined ethanol  
10  
11  
12 400 organosolve/hydrothermal treatment (194% improvement) (Charnnok et al., 2020). Secondly,  
13  
14  
15 401 the lack of economical pretreatment technologies further hindered the practical utilization of  
16  
17  
18 402 wood waste AD. The proposed method leverages natural systems without requiring  
19  
20  
21 403 significant additional economic inputs, with the potential to be highly cost-effective as a  
22  
23  
24 404 result. By harnessing the inherent capabilities of natural forest processes, this nature-based  
25  
26  
27 405 approach offers a practical and scalable solution for enhancing the efficiency of AD  
28  
29  
30 406 operations for wood waste.

31  
32 407 The economic viability of AD with wood waste has been thoroughly described in the  
33  
34  
35 408 literature. Teghammar et al. (2014) conducted an economic assessment of biogas production  
36  
37  
38 409 from forest residues with pretreatment enhancement, showing that an AD plant processing  
39  
40  
41 410 50000 tons dry weight of forest residues per year is economically viable. The techno-  
42  
43  
44 411 economic assessment showed that methanol pretreatment was more financially acceptable  
45  
46  
47 412 than acetic acid and ethanol, and the capital investment for operating an AD plant treating  
48  
49  
50 413 20,000 tons of forest residues per year could be recouped within eight years (Kabir et al.,  
51  
52  
53 414 2015). Moreover, AD was shown to be an environmentally friendly method of recovering  
54  
55  
56 415 energy from wood waste compared to other management processes through life cycle  
57  
58  
59 416 assessment analysis (da Costa et al., 2020; Liang et al., 2017; Nogueira et al., 2021). To  
60  
61 417 further explore the differences between all DC samples and find the best DC for application  
62  
63  
64  
65

1 418 in AD, a net profit analysis was conducted. Considering that the AD process was the same  
2  
3  
4 419 for all DC samples, the net energy output could be calculated from the electricity input of  
5  
6 420 grinding the samples and the methane production. According to Wu et al. (2016), the calorific  
7  
8  
9 421 value of methane is 11.06 kWh/m<sup>3</sup>. As shown in Fig. 6, DC3 had a high net energy output,  
10  
11  
12 422 which implies that this stage has the potential to be used in AD plants. ~~It is worth noting that~~  
13  
14  
15 423 ~~does not consider the effect of subsidies or economies of scale.~~ For fire protection reasons  
16  
17  
18 424 and energy considerations, the forest residues should not be retained in the forest.  
19  
20  
21 425 Unfortunately, the direct recycling of these forest residues also may result in the removal of  
22  
23  
24 426 minerals that would otherwise fertilize the soil and promote the future growth of trees  
25  
26  
27 427 (Grotsky et al., 2018). These results may provide guidance on specific collection times for  
28  
29  
30 428 forest residues in practice. This study proposes to collect DC3 samples, which satisfies the  
31  
32  
33 429 requirement of releasing minerals from the wood waste to maintain the forest ecology while  
34  
35  
36 430 keeping the highest methane yield.

37  
38 431 To better utilize this nature-based approach, more detailed experiments and analyses are  
39  
40  
41 432 still needed to bridge the following issues. Firstly, more wood samples of various species are  
42  
43  
44 433 needed to verify the generalizability of this approach, as well as to investigate the duration  
45  
46  
47 434 for forest residues to reach DC3 in different forest environments to facilitate the collection  
48  
49  
50 435 of samples. Secondly, there is a loss of mass in the degradation process of forest residues  
51  
52  
53 436 (Oberle et al., 2020; Seibold et al., 2021), so it is important to explore how mass loss varies  
54  
55  
56 437 with DC. Thirdly, anaerobic co-digestion of wood waste with other organic wastes can  
57  
58  
59 438 balance the carbon to nitrogen ratio of the substrate and enhance methane production (Li et  
60  
61  
62 439 al., 2019; Oh et al., 2018). Additionally, the combination of other pretreatment technologies

1 440 can improve substrate availability to microorganisms in AD (Wang et al., 2024; Zhang et al.,  
2  
3  
4 441 2017). Therefore, anaerobic co-digestion of different DC wood waste and other organic  
5  
6 442 wastes and the possibility of combining this nature-based approach with other pretreatments  
7  
8  
9 443 need to be explored for maximizing energy recovery from wood wastes.  
10

## 11 **4 Conclusion**

12 444

13  
14  
15 445 This study investigated a novel nature-based approach to promote AD application of  
16  
17  
18 446 forest residues. Specifically, this approach exploited the lignocellulose degradation processes  
19  
20  
21 447 inherent in forest ecosystems, combined with a strategic collection to maximize the AD  
22  
23  
24 448 potential of forest residues. Based on the experimental results, the following conclusions can  
25  
26  
27 449 be drawn:

- 28  
29 450 1) The texture of the forest residues was softened by processing with this nature-based  
30  
31  
32 451 approach, making them easier to be shredded. The SEC results showed that the energy  
33  
34  
35 452 required to grind the same dry weight of wood sample decreased with increasing DC.  
36  
37  
38 453 A subsequent particle size analysis showed that wood samples with higher DC had  
39  
40  
41 454 smaller average particle sizes after grinding.  
42  
43
- 44 455 2) High DC wood samples had higher WEOC, lower cellulose crystallinity, and a more  
45  
46  
47 456 suitable carbon to nitrogen ratio for AD. Although the lignin content was relatively  
48  
49  
50 457 higher in high DC wood samples, the recalcitrance of their lignocellulosic structure  
51  
52  
53 458 was disrupted. These changes are expected to lead to enhanced methane production  
54  
55  
56 459 because of a breakdown of the lignocellulosic structure, increasing access to  
57  
58  
59 460 microorganisms involved in AD.  
60  
61  
62  
63  
64  
65

1 461 3) A preliminary test of this nature-based approach by AD experiments showed that  
2  
3  
4 462 wood samples from DC 1 had the lowest methane yield, while DC 3 samples had the  
5  
6 463 highest, with a notable 160% increase compared to DC 1. In addition, the net profit  
7  
8  
9 464 analysis indicated that wood samples from DC 3 to DC 5 had a net energy output  
10  
11  
12 465 when applied in AD, with the net energy output being relatively high in DC 3 and DC  
13  
14  
15 466 4. Therefore, these results imply that DC3 might be the optimal level of decay for  
16  
17  
18 467 forest residues collection.

19  
20  
21 468 This study is the first to introduce the concept of a nature-based approach to enhance the  
22  
23  
24 469 AD performance of forest residues, and to explore it in detail experimentally. This approach,  
25  
26  
27 470 when combined with a strategic collection method, can significantly improve the overall  
28  
29  
30 471 profitability and sustainability of bioenergy production from forest residues. Furthermore,  
31  
32  
33 472 the feasibility of more forest ecosystems in boosting the AD application of forest residues  
34  
35  
36 473 should be further explored, as this can broaden the applications of this novel nature-based  
37  
38  
39 474 approach.

## 40 41 475 **Acknowledgments**

42  
43  
44 476 The authors gratefully acknowledge financial support from the China Scholarship  
45  
46  
47 477 Council (CSC) for Zhenghui Gao (CSC No. 202006760088). Sapsford, Cleall and Harbottle  
48  
49  
50 478 were supported by the UK Research and Innovation-funded project ‘ASPIRE – Accelerated  
51  
52  
53 479 Supergene Processes in Repository Engineering’ (EP/T03100X/1).

## 54 55 480 **Reference**

56  
57 481 Alexandropoulou, M., Antonopoulou, G., Ntaikou, I., Lyberatos, G., 2017. Fungal Pretreatment of Willow  
58  
59 482 Sawdust with *Abortiporus biennis* for Anaerobic Digestion: Impact of an External Nitrogen Source.  
60 483 *Sustainability* 9, 130. <https://doi.org/10.3390/su9010130>

- 484 Ali, S.S., Abomohra, A.E.-F., Sun, J., 2017. Effective bio-pretreatment of sawdust waste with a novel microbial  
485 consortium for enhanced biomethanation. *Bioresour. Technol.* 238, 425–432.  
486 <https://doi.org/10.1016/j.biortech.2017.03.187>
- 487 Antonopoulou, G., Gavala, H.N., Skiadas, I.V., Lyberatos, G., 2015. The Effect of Aqueous Ammonia Soaking  
488 Pretreatment on Methane Generation Using Different Lignocellulosic Biomasses. *Waste Biomass  
489 Valorization* 6, 281–291. <https://doi.org/10.1007/s12649-015-9352-9>
- 490 Atelge, M.R., Atabani, A.E., Banu, J.R., Krisa, D., Kaya, M., Eskicioglu, C., Kumar, G., Lee, C., Yildiz, Y.Ş.,  
491 Unalan, S., Mohanasundaram, R., Duman, F., 2020. A critical review of pretreatment technologies to  
492 enhance anaerobic digestion and energy recovery. *Fuel* 270, 117494.  
493 <https://doi.org/10.1016/j.fuel.2020.117494>
- 494 Awoyale, A.A., Lokhat, D., 2021. Experimental determination of the effects of pretreatment on selected  
495 Nigerian lignocellulosic biomass in bioethanol production. *Sci. Rep.* 11, 557.  
496 <https://doi.org/10.1038/s41598-020-78105-8>
- 497 Charnnok, B., Sawangkeaw, R., Chairapat, S., 2020. Integrated process for the production of fermentable sugar  
498 and methane from rubber wood. *Bioresour. Technol.* 302, 122785.  
499 <https://doi.org/10.1016/j.biortech.2020.122785>
- 500 D' Silva, T.C., Isha, A., Verma, S., Shirsath, G., Chandra, R., Vijay, V.K., Subbarao, P.M.V., Kovács, K.L.,  
501 2022. Anaerobic co-digestion of dry fallen leaves, fruit/vegetable wastes and cow dung without an  
502 active inoculum – A biomethane potential study. *Bioresour. Technol. Rep.* 19, 101189.  
503 <https://doi.org/10.1016/j.biteb.2022.101189>
- 504 da Costa, T.P., Quinteiro, P., Arroja, L., Dias, A.C., 2020. Environmental comparison of forest biomass residues  
505 application in Portugal: Electricity, heat and biofuel. *Renew. Sustain. Energy Rev.* 134, 110302.  
506 <https://doi.org/10.1016/j.rser.2020.110302>
- 507 Dai, B., Guo, X., Yuan, D., Xu, J., 2018. Comparison of Different Pretreatments of Rice Straw Substrate to  
508 Improve Biogas Production. *Waste Biomass Valorization* 9, 1503–1512.  
509 <https://doi.org/10.1007/s12649-017-9950-9>
- 510 Dai, X., Hua, Y., Dai, L., Cai, C., 2019. Particle size reduction of rice straw enhances methane production under  
511 anaerobic digestion. *Bioresour. Technol.* 293, 122043. <https://doi.org/10.1016/j.biortech.2019.122043>
- 512 Darmawan, S., Wistara, N.J., Pari, G., Maddu, A., Syafii, W., 2016. Characterization of Lignocellulosic  
513 Biomass as Raw Material for the Production of Porous Carbon-based Materials. *BioResources* 11,  
514 3561–3574.
- 515 Díez, D., Urueña, A., Piñero, R., Barrio, A., Tamminen, T., 2020. Determination of Hemicellulose, Cellulose,  
516 and Lignin Content in Different Types of Biomasses by Thermogravimetric Analysis and  
517 Pseudocomponent Kinetic Model (TGA-PKM Method). *Processes* 8, 1048.  
518 <https://doi.org/10.3390/pr8091048>
- 519 Eom, T., Chairapat, S., Charnnok, B., 2019. Enhanced enzymatic hydrolysis and methane production from  
520 rubber wood waste using steam explosion. *J. Environ. Manage.* 235, 231–239.  
521 <https://doi.org/10.1016/j.jenvman.2019.01.041>
- 522 Gao, Z., Alshehri, K., Li, Y., Qian, H., Sapsford, D., Cleall, P., Harbottle, M., 2022. Advances in biological  
523 techniques for sustainable lignocellulosic waste utilization in biogas production. *Renew. Sustain.  
524 Energy Rev.* 170, 112995. <https://doi.org/10.1016/j.rser.2022.112995>
- 525 Gao, Z., Cui, T., Qian, H., Sapsford, D.J., Cleall, P.J., Harbottle, M.J., 2024a. Can wood waste be a feedstock  
526 for anaerobic digestion? A machine learning assisted *meta-analysis*. *Chem. Eng. J.* 150496.  
527 <https://doi.org/10.1016/j.cej.2024.150496>

- 528 Gao, Z., Muazz-Uz-Salam, S., Sapsford, D., Cleall, P., Harbottle, M., 2023. Application of natural  
1 529 biodelignification systems in forest soil for enhanced anaerobic digestion potential of wood waste.  
2 530 Presented at the Proceedings of the 9th International Congress on Environmental Geotechnics  
3 531 (ICEG2023), pp. 13–22. <https://doi.org/10.53243/ICEG2023-59>  
4 532 Gao, Z., Qian, H., Cui, T., Ren, Z., Wang, X., 2024b. Comprehensive *meta*-analysis reveals the impact of non-  
5 533 biodegradable plastic pollution on methane production in anaerobic digestion. *Chem. Eng. J.* 484,  
6 534 149703. <https://doi.org/10.1016/j.cej.2024.149703>  
7 535 Gao, Z., Ren, Z., Cui, T., Fu, Y., 2025. Machine learning-based analysis of microplastic-induced changes in  
8 536 anaerobic digestion parameters influencing methane yield. *J. Environ. Manage.* 377, 124627.  
9 537 <https://doi.org/10.1016/j.jenvman.2025.124627>  
10 538 Garvie, L.C., Roxburgh, S.H., Ximenes, F.A., 2021. Greenhouse Gas Emission Offsets of Forest Residues for  
11 539 Bioenergy in Queensland, Australia. *Forests* 12, 1570. <https://doi.org/10.3390/f12111570>  
12 540 Grodsky, S.M., Moorman, C.E., Fritts, S.R., Campbell, J.W., Sorenson, C.E., Bertone, M.A., Castleberry, S.B.,  
13 541 Wigley, T.B., 2018. Invertebrate community response to coarse woody debris removal for bioenergy  
14 542 production from intensively managed forests. *Ecol. Appl.* 28, 135–148.  
15 543 <https://doi.org/10.1002/eap.1634>  
16 544 Hashemi, S., Solli, L., Aasen, R., Lamb, J.J., Horn, S.J., Lien, K.M., 2022. Stimulating biogas production from  
17 545 steam-exploded birch wood using Fenton reaction and fungal pretreatment. *Bioresour. Technol.* 366,  
18 546 128190. <https://doi.org/10.1016/j.biortech.2022.128190>  
19 547 He, C., Song, H., Liu, L., Li, P., Kumar Awasthi, M., Xu, G., Zhang, Q., Jiao, Y., Chang, C., Yang, Y., 2022.  
20 548 Enhancement of methane production by anaerobic digestion of corn straw with hydrogen-nanobubble  
21 549 water. *Bioresour. Technol.* 344, 126220. <https://doi.org/10.1016/j.biortech.2021.126220>  
22 550 Isha, A., D' Silva, T.C., Subbarao, P.M.V., Chandra, R., Vijay, V.K., 2021. Stabilization of anaerobic digestion  
23 551 of kitchen wastes using protein-rich additives: Study of process performance, kinetic modelling and  
24 552 energy balance. *Bioresour. Technol.* 337, 125331. <https://doi.org/10.1016/j.biortech.2021.125331>  
25 553 Ji, J.-L., Chen, F., Liu, S., Yang, Y., Hou, C., Wang, Y.-Z., 2022. Co-production of biogas and humic acid using  
26 554 rice straw and pig manure as substrates through solid-state anaerobic fermentation and subsequent  
27 555 aerobic composting. *J. Environ. Manage.* 320, 115860.  
28 556 <https://doi.org/10.1016/j.jenvman.2022.115860>  
29 557 Kabir, M.M., Rajendran, K., Taherzadeh, M.J., Sárvári Horváth, I., 2015. Experimental and economical  
30 558 evaluation of bioconversion of forest residues to biogas using organosolv pretreatment. *Bioresour.*  
31 559 *Technol.* 178, 201–208. <https://doi.org/10.1016/j.biortech.2014.07.064>  
32 560 Kamarudin, S.N.C., Jainal, M.S., Azizan, A., Safaai, N.S.M., Daud, A.R.M., 2014. Mechanical Pretreatment  
33 561 of Lignocellulosic Biomass for Biofuel Production. *Appl. Mech. Mater.* 625, 838–841.  
34 562 <https://doi.org/10.4028/www.scientific.net/AMM.625.838>  
35 563 Karami, K., Karimi, K., Mirmohamadsadeghi, S., Kumar, R., 2022. Mesophilic aerobic digestion: An efficient  
36 564 and inexpensive biological pretreatment to improve biogas production from highly-recalcitrant  
37 565 pinewood. *Energy* 239, 122361. <https://doi.org/10.1016/j.energy.2021.122361>  
38 566 Kumar, S., D' Silva, T.C., Chandra, R., Malik, A., Vijay, V.K., Misra, A., 2021. Strategies for boosting  
39 567 biomethane production from rice straw: A systematic review. *Bioresour. Technol. Rep.* 15, 100813.  
40 568 <https://doi.org/10.1016/j.biteb.2021.100813>  
41 569 Kumar, S., Gandhi, P., Yadav, M., Paritosh, K., Pareek, N., Vivekanand, V., 2019. Weak alkaline treatment of  
42 570 wheat and pearl millet straw for enhanced biogas production and its economic analysis. *Renew. Energy*  
43 571 139, 753–764. <https://doi.org/10.1016/j.renene.2019.02.133>

- 572 Kurvits, V., Ots, K., Kangur, A., Korjus, H., Muiste, P., 2020. Assessment of load and quality of logging  
1 573 residues from clear-felling areas in Järvselja: a case study from Southeast Estonia. *Cent. Eur. For. J.*  
2 574 66, 3–11. <https://doi.org/10.2478/forj-2019-0022>
- 3 575 Lai, Z., Chen, D., Jiang, E., Zhao, L., Vallejo, L.E., Zhou, W., 2021. Effect of fractal particle size distribution  
4 576 on the mobility of dry granular flows. *AIP Adv.* 11, 095113. <https://doi.org/10.1063/5.0065051>
- 5 577 Lee, E., Han, H.-S., 2017. Air Curtain Burners: A Tool for Disposal of Forest Residues. *Forests* 8, 296.  
6 578 <https://doi.org/10.3390/f8080296>
- 7 579 Li, R., Tan, W., Zhao, X., Dang, Q., Song, Q., Xi, B., Zhang, X., 2019. Evaluation on the Methane Production  
8 580 Potential of Wood Waste Pretreated with NaOH and Co-Digested with Pig Manure. *Catalysts* 9, 539.  
9 581 <https://doi.org/10.3390/catal9060539>
- 10 582 Liang, S., Gu, H., Bergman, R.D., 2017. Life cycle assessment of cellulosic ethanol and biomethane production  
11 583 from forest residues. *BioResources* 12, 7873–7883. <https://doi.org/10.15376/biores.12.4.7873-7883>
- 12 584 Liu, X., Hilgsmann, S., Gourdon, R., Bayard, R., 2017. Anaerobic digestion of lignocellulosic biomasses  
13 585 pretreated with *Ceriporiopsis subvermispora*. *J. Environ. Manage.* 193, 154–162.  
14 586 <https://doi.org/10.1016/j.jenvman.2017.01.075>
- 15 587 Liu, X., Zicari, S.M., Liu, G., Li, Y., Zhang, R., 2015. Pretreatment of wheat straw with potassium hydroxide  
16 588 for increasing enzymatic and microbial degradability. *Bioresour. Technol.* 185, 150–157.  
17 589 <https://doi.org/10.1016/j.biortech.2015.02.047>
- 18 590 Lübken, M., Gehring, T., Wichern, M., 2010. Microbiological fermentation of lignocellulosic biomass: current  
19 591 state and prospects of mathematical modeling. *Appl. Microbiol. Biotechnol.* 85, 1643–1652.  
20 592 <https://doi.org/10.1007/s00253-009-2365-1>
- 21 593 Luo, L., Qu, Y., Gong, W., Qin, L., Li, W., Sun, Y., 2021. Effect of Particle Size on the Aerobic and Anaerobic  
22 594 Digestion Characteristics of Whole Rice Straw. *Energies* 14, 3960.  
23 595 <https://doi.org/10.3390/en14133960>
- 24 596 Manikandan, S., Vickram, S., Sirohi, R., Subbaiya, R., Krishnan, R.Y., Karmegam, N., Sumathijones, C.,  
25 597 Rajagopal, R., Chang, S.W., Ravindran, B., Awasthi, M.K., 2023. Critical review of biochemical  
26 598 pathways to transformation of waste and biomass into bioenergy. *Bioresour. Technol.* 372, 128679.  
27 599 <https://doi.org/10.1016/j.biortech.2023.128679>
- 28 600 Mao, C., Wang, X., Xi, J., Feng, Y., Ren, G., 2017. Linkage of kinetic parameters with process parameters and  
29 601 operational conditions during anaerobic digestion. *Energy* 135, 352–360.  
30 602 <https://doi.org/10.1016/j.energy.2017.06.050>
- 31 603 Matsakas, L., Rova, U., Christakopoulos, P., 2015. Sequential parametric optimization of methane production  
32 604 from different sources of forest raw material. *Front. Microbiol.* 6.
- 33 605 Miao, Z., Grift, T.E., Hansen, A.C., Ting, K.C., 2011. Energy requirement for comminution of biomass in  
34 606 relation to particle physical properties. *Ind. Crops Prod.* 33, 504–513.  
35 607 <https://doi.org/10.1016/j.indcrop.2010.12.016>
- 36 608 Mo, X., Wang, M., Wang, Y., Zhang, P., Zhang, A., Kong, D., Zeng, H., Wang, J., 2022. High content and  
37 609 distinct spectroscopic characteristics of water-extractable organic matter in rhizosphere soils in a  
38 610 semiarid grassland. *Rhizosphere* 23, 100553. <https://doi.org/10.1016/j.rhisph.2022.100553>
- 39 611 Mohsenzadeh, A., Jeihanipour, A., Karimi, K., Taherzadeh, M.J., 2012. Alkali pretreatment of softwood spruce  
40 612 and hardwood birch by NaOH/thiourea, NaOH/urea, NaOH/urea/thiourea, and NaOH/PEG to improve  
41 613 ethanol and biogas production. *J. Chem. Technol. Biotechnol.* 87, 1209–1214.  
42 614 <https://doi.org/10.1002/jctb.3695>

- 1 615 Moiceanu, G., Paraschiv, G., Voicu, G., Dinca, M., Negoita, O., Chitoiu, M., Tudor, P., 2019. Energy  
2 616 Consumption at Size Reduction of Lignocellulose Biomass for Bioenergy. *Sustainability* 11, 2477.  
3 617 <https://doi.org/10.3390/su11092477>
- 4 618 Molenda, M., Horabik, J., Parafiniuk, P., Oniszczyk, A., Bańda, M., Wajs, J., Gondek, E., Chutkowski, M.,  
5 619 Lisowski, A., Wiącek, J., Stasiak, M., 2021. Mechanical and Combustion Properties of Agglomerates  
6 620 of Wood of Popular Eastern European Species. *Materials* 14, 2728.  
7 621 <https://doi.org/10.3390/ma14112728>
- 8 622 Muaz-Us-Salam, S., Cleall, P.J., Harbottle, M.J., 2020. Application of enzymatic and bacterial  
9 623 biodelignification systems for enhanced breakdown of model lignocellulosic wastes. *Sci. Total*  
10 624 *Environ.* 728, 138741. <https://doi.org/10.1016/j.scitotenv.2020.138741>
- 11 625 Mulat, D.G., Huerta, S.G., Kalyani, D., Horn, S.J., 2018. Enhancing methane production from lignocellulosic  
12 626 biomass by combined steam-explosion pretreatment and bioaugmentation with cellulolytic bacterium  
13 627 *Caldicellulosiruptor bescii*. *Biotechnol. Biofuels* 11, 19. <https://doi.org/10.1186/s13068-018-1025-z>
- 14 628 Nicholls, D.L., Halbrook, J.M., Benedum, M.E., Han, H.-S., Lowell, E.C., Becker, D.R., Barbour, R.J., 2018.  
15 629 Socioeconomic Constraints to Biomass Removal from Forest Lands for Fire Risk Reduction in the  
16 630 Western U.S. *Forests* 9, 264. <https://doi.org/10.3390/f9050264>
- 17 631 Nogueira, G.P., McManus, M.C., Leak, D.J., Franco, T.T., Oliveira de Souza Dias, M., Nakao Cavaliero, C.K.,  
18 632 2021. Are eucalyptus harvest residues a truly burden-free biomass source for bioenergy? A deeper  
19 633 look into biorefinery process design and Life Cycle Assessment. *J. Clean. Prod.* 299, 126956.  
20 634 <https://doi.org/10.1016/j.jclepro.2021.126956>
- 21 635 Oberle, B., Lee, M.R., Myers, J.A., Osazuwa-Peters, O.L., Spasojevic, M.J., Walton, M.L., Young, D.F., Zanne,  
22 636 A.E., 2020. Accurate forest projections require long-term wood decay experiments because plant trait  
23 637 effects change through time. *Glob. Change Biol.* 26, 864–875. <https://doi.org/10.1111/gcb.14873>
- 24 638 Oh, J.-I., Lee, J., Lin, K.-Y.A., Kwon, E.E., Fai Tsang, Y., 2018. Biogas production from food waste via  
25 639 anaerobic digestion with wood chips. *Energy Environ.* 29, 1365–1372.  
26 640 <https://doi.org/10.1177/0958305X18777234>
- 27 641 Pergola, M.T., Saulino, L., Castellaneta, M., Rita, A., Pecora, G., Cozzi, M., Moretti, N., Pericolo, O., Pierangeli,  
28 642 D., Romano, S., Viccaro, M., Ripullone, F., 2022. Towards sustainable management of forest residues  
29 643 in the southern Apennine Mediterranean mountain forests: a scenario-based approach. *Ann. For. Sci.*  
30 644 79, 14. <https://doi.org/10.1186/s13595-022-01128-w>
- 31 645 Petritan, I.C., Mihăilă, V.-V., Yuste, J.C., Bouriaud, O., Petritan, A.M., 2023. Deadwood density, C stocks and  
32 646 their controlling factors in a beech-silver fir mixed virgin European forest. *For. Ecol. Manag.* 539,  
33 647 121007. <https://doi.org/10.1016/j.foreco.2023.121007>
- 34 648 Piątek, M., Lisowski, A., Kasprzycka, A., Lisowska, B., 2016. The dynamics of an anaerobic digestion of crop  
35 649 substrates with an unfavourable carbon to nitrogen ratio. *Bioresour. Technol.* 216, 607–612.  
36 650 <https://doi.org/10.1016/j.biortech.2016.05.122>
- 37 651 Provenzano, M.R., Malerba, A.D., Pezzolla, D., Gigliotti, G., 2014. Chemical and spectroscopic  
38 652 characterization of organic matter during the anaerobic digestion and successive composting of pig  
39 653 slurry. *Waste Manag.* 34, 653–660. <https://doi.org/10.1016/j.wasman.2013.12.001>
- 40 654 Rabot, E., Wiesmeier, M., Schlüter, S., Vogel, H.-J., 2018. Soil structure as an indicator of soil functions: A  
41 655 review. *Geoderma* 314, 122–137. <https://doi.org/10.1016/j.geoderma.2017.11.009>
- 42 656 Rego, F., Soares Dias, A.P., Casquilho, M., Rosa, F.C., Rodrigues, A., 2019. Fast determination of  
43 657 lignocellulosic composition of poplar biomass by thermogravimetry. *Biomass Bioenergy* 122, 375–  
44 658 380. <https://doi.org/10.1016/j.biombioe.2019.01.037>

- 659 Rice, E.W., Baird, R.B., Eaton, A.D., 2017. Standard Methods for the Examination of Water and Wastewater,  
1 23rd edn. American Public Health Association, American Water Works Association, Water  
2 Environment Federation (2017). ISBN: 9780875532875.  
3 661
- 4 662 Salehian, P., Karimi, K., Zilouei, H., Jeihanipour, A., 2013. Improvement of biogas production from pine wood  
5 by alkali pretreatment. *Fuel* 106, 484–489. <https://doi.org/10.1016/j.fuel.2012.12.092>  
6 663
- 7 664 Seibold, S., Rammer, W., Hothorn, T., Seidl, R., Ulyshen, M.D., Lorz, J., Cadotte, M.W., Lindenmayer, D.B.,  
8 Adhikari, Y.P., Aragón, R., Bae, S., Baldrian, P., Barimani Varandi, H., Barlow, J., Bässler, C.,  
9 665 Beauchêne, J., Berenguer, E., Bergamin, R.S., Birkemoe, T., Boros, G., Brandl, R., Brustel, H., Burton,  
10 666 P.J., Cakpo-Tossou, Y.T., Castro, J., Cateau, E., Cobb, T.P., Farwig, N., Fernández, R.D., Firn, J., Gan,  
11 667 K.S., González, G., Gossner, M.M., Habel, J.C., Hébert, C., Heibl, C., Heikkala, O., Hemp, A., Hemp,  
12 668 C., Hjältén, J., Hotes, S., Kouki, J., Lachat, T., Liu, J., Liu, Y., Luo, Y.-H., Macandog, D.M., Martina,  
13 669 P.E., Mukul, S.A., Nachin, B., Nisbet, K., O’Halloran, J., Oxbrough, A., Pandey, J.N., Pavlíček, T.,  
14 670 Pawson, S.M., Rakotondranary, J.S., Ramanamanjato, J.-B., Rossi, L., Schmidl, J., Schulze, M.,  
15 671 Seaton, S., Stone, M.J., Stork, N.E., Suran, B., Sverdrup-Thygeson, A., Thorn, S., Thyagarajan, G.,  
16 672 Wardlaw, T.J., Weisser, W.W., Yoon, S., Zhang, N., Müller, J., 2021. The contribution of insects to  
17 673 global forest deadwood decomposition. *Nature* 597, 77–81. <https://doi.org/10.1038/s41586-021-03740-8>  
18 674  
19 675
- 20 676 Shorohova, E., Kapitsa, E., Kuznetsov, A., Kuznetsova, S., Lopes de Gerenuy, V., Kaganov, V., Kurganova, I.,  
21 677 2021. Decay classes of coarse woody debris in a lowland Dipterocarp forest: implications for volume,  
22 678 density, and carbon estimates. *Biotropica* 53, 879–887. <https://doi.org/10.1111/btp.12947>  
23 679
- 24 680 Song, C., Cai, F., Yang, S., Wang, L., Liu, G., Chen, C., 2024. Machine learning-based prediction of methane  
25 681 production from lignocellulosic wastes. *Bioresour. Technol.* 393, 129953.  
26 682 <https://doi.org/10.1016/j.biortech.2023.129953>  
27 683
- 28 684 Tarasov, D., Leitch, M., Fatehi, P., 2018. Lignin–carbohydrate complexes: properties, applications, analyses,  
29 685 and methods of extraction: a review. *Biotechnol. Biofuels* 11, 269. <https://doi.org/10.1186/s13068-018-1262-1>  
30 686
- 31 687 Tatti, D., Fatton, V., Sartori, L., Gobat, J.-M., Le Bayon, R.-C., 2018. What does ‘lignoform’ really mean? *Appl. Soil Ecol., HUMUSICA* 3 - Reviews, Applications, Tools 123, 632–645. <https://doi.org/10.1016/j.apsoil.2017.06.037>  
32 688
- 33 689 Teghammar, A., Forgács, G., Sárvári Horváth, I., Taherzadeh, M.J., 2014. Techno-economic study of NMMO  
34 690 pretreatment and biogas production from forest residues. *Appl. Energy* 116, 125–133. <https://doi.org/10.1016/j.apenergy.2013.11.053>  
35 691
- 36 692 Tian, Y., Zhang, H., Mi, X., Wang, L., Zhang, L., Ai, Y., 2016. Research on anaerobic digestion of corn stover  
37 693 enhanced by dilute acid pretreatment: Mechanism study and potential utilization in practical  
38 694 application. *J. Renew. Sustain. Energy* 8, 023103. <https://doi.org/10.1063/1.4945570>  
39 695
- 40 696 Wang, W., Jiang, M.-F., Hsu, J.-R., Guo, G.-L., 2024. Integrated alkaline-solid/liquid separation-thermal  
41 697 multiple-step pretreatment of lignocellulosic biomass for biogas production enhancement. *Biomass Convers. Biorefinery*. <https://doi.org/10.1007/s13399-024-05288-9>  
42 698
- 43 699 Wang, Z.-W., Xu, F., Manchala, K.R., Sun, Y., Li, Y., 2016. Fractal-like kinetics of the solid-state anaerobic  
44 700 digestion. *Waste Manag.* 53, 55–61. <https://doi.org/10.1016/j.wasman.2016.04.019>  
45 701
- 46 702 Wu, A., Lovett, D., McEwan, M., Cecelja, F., Chen, T., 2016. A spreadsheet calculator for estimating biogas  
47 703 production and economic measures for UK-based farm-fed anaerobic digesters. *Bioresour. Technol.* 220, 479–489. <https://doi.org/10.1016/j.biortech.2016.08.103>  
48 704  
49 705

1  
2  
3  
4  
5  
6  
7  
8  
9  
10  
11  
12  
13  
14  
15  
16  
17  
18  
19  
20  
21  
22  
23  
24  
25  
26  
27  
28  
29  
30  
31  
32  
33  
34  
35  
36  
37  
38  
39  
40  
41  
42  
43  
44  
45  
46  
47  
48  
49  
50  
51  
52  
53  
54  
55  
56  
57  
58  
59  
60  
61  
62  
63  
64  
65

702 Xing, M., Li, X., Yang, J., Huang, Z., Lu, Y., 2012. Changes in the chemical characteristics of water-extracted  
703 organic matter from vermicomposting of sewage sludge and cow dung. *J. Hazard. Mater.* 205–206,  
704 24–31. <https://doi.org/10.1016/j.jhazmat.2011.11.070>

705 Xu, S., Selvam, A., Wong, J.W.C., 2014. Optimization of micro-aeration intensity in acidogenic reactor of a  
706 two-phase anaerobic digester treating food waste. *Waste Manag.* 34, 363–369.  
707 <https://doi.org/10.1016/j.wasman.2013.10.038>

708 Xu, W., Fu, S., Yang, Z., Lu, J., Guo, R., 2018. Improved methane production from corn straw by microaerobic  
709 pretreatment with a pure bacteria system. *Bioresour. Technol.* 259, 18–23.  
710 <https://doi.org/10.1016/j.biortech.2018.02.046>

711 Yoon, S.-M., Kim, M.-J., Hwang, W.-J., Lee, H.-M., Park, Y., Son, D.-W., Kim, Y.-S., Choi, Y.-S., 2023.  
712 Natural durability and fungal diversity of five wood species in a field-test site in Jeongseon, Korea.  
713 *Holzforschung* 77, 577–584. <https://doi.org/10.1515/hf-2023-0034>

714 Zhang, B., Ji, M., Wang, F., Li, R., Zhang, K., Yin, X., Li, Q., 2017. Damage of EPS and cell structures and  
715 improvement of high-solid anaerobic digestion of sewage sludge by combined (Ca(OH)<sub>2</sub> + multiple-  
716 transducer ultrasonic) pretreatment. *RSC Adv.* 7, 22706–22714. <https://doi.org/10.1039/C7RA01060E>

717 Zhang, D., Cai, C., Zhu, J., 2021. Changes of Soil Water–Stable Aggregates after Rice–Crawfish Rotation in  
718 Low-lying Paddy Fields: A Case Study in Jiangnan Plain of China. *Commun. Soil Sci. Plant Anal.* 52,  
719 2358–2372. <https://doi.org/10.1080/00103624.2021.1928169>

720 Zhu, J.Y., Sabo, R., Luo, X., 2011. Integrated production of nano-fibrillated cellulose and cellulosic biofuel  
721 (ethanol) by enzymatic fractionation of wood fibers. *Green Chem.* 13, 1339–1344.  
722 <https://doi.org/10.1039/C1GC15103G>

723

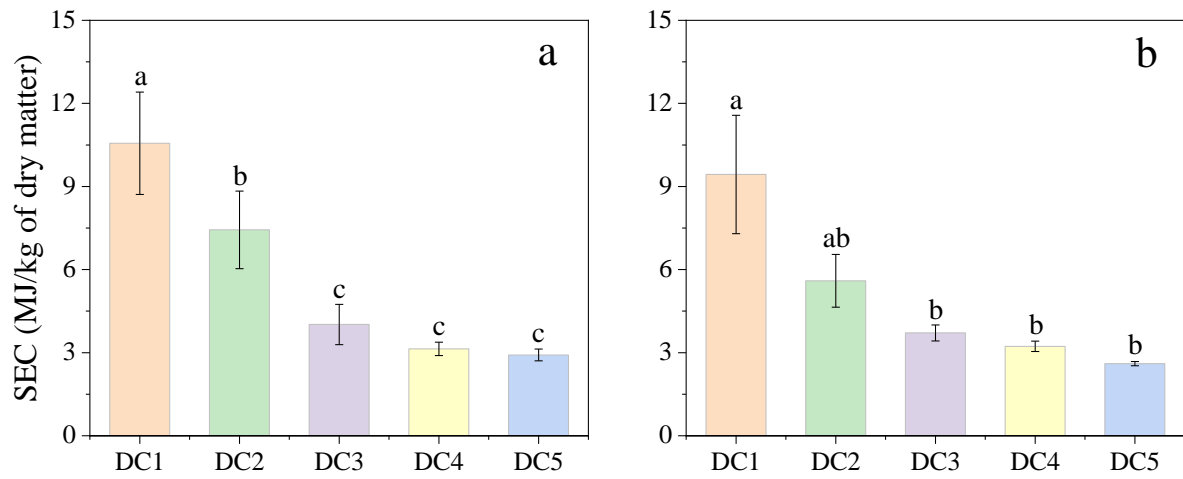


Fig. 1. Specific energy consumption (SEC) for grinding wood samples from five decay classes, (a) Birch; (b) Ash. Different lowercase letters above each column indicate significant differences (columns with different letters are statistically significantly different from one another).

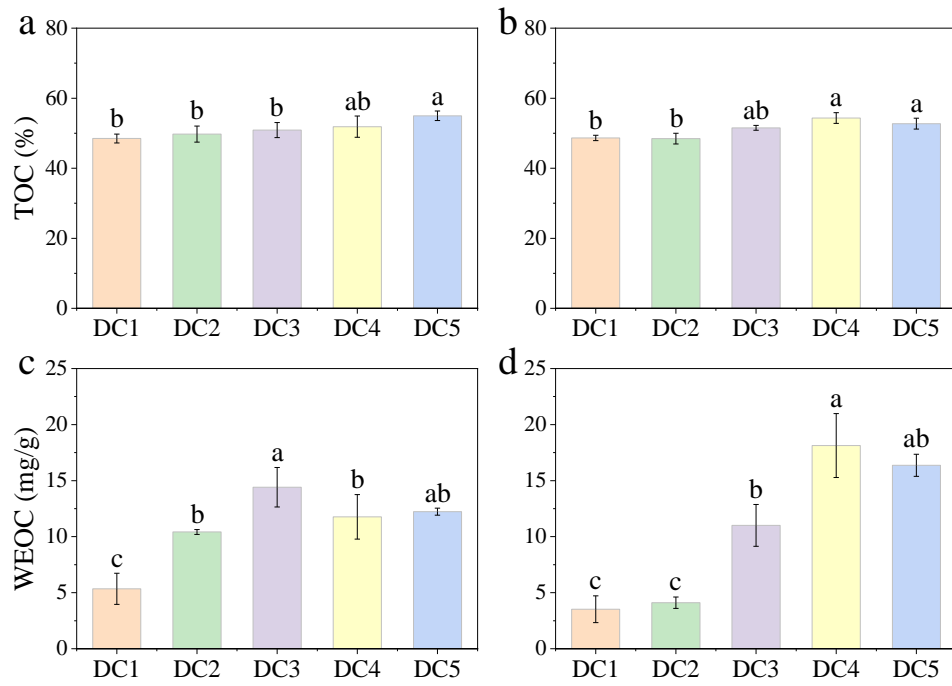


Fig. 2. Different categories of organic carbon from five decay classes wood samples. The total organic carbon (TOC) content of (a) Birch and (b) Ash, and water extractable organic carbon (WEOC) of (c) Birch and (d) Ash. Different lowercase letters above columns indicate a difference at a 0.05 level.

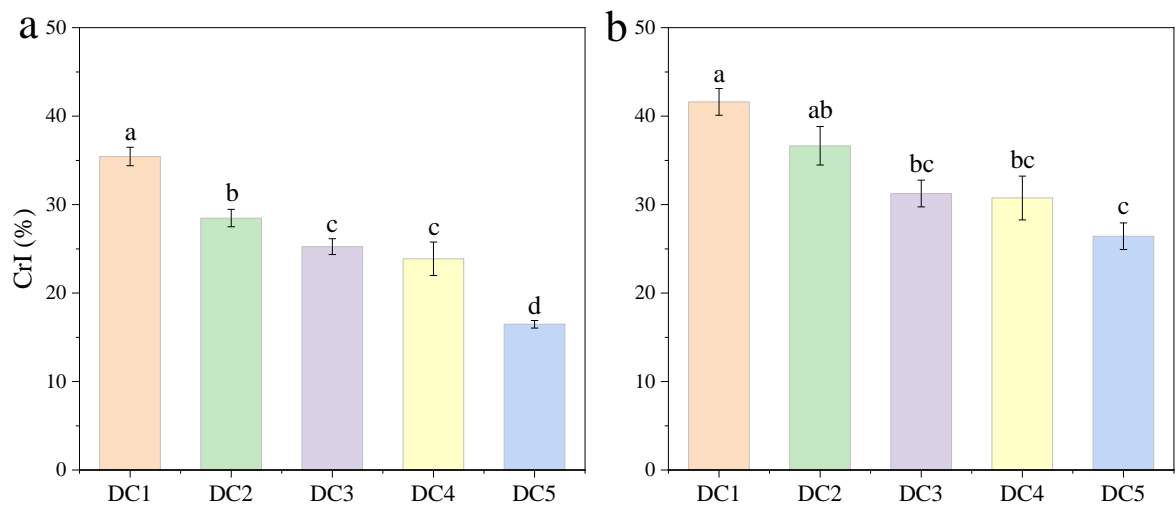


Fig. 3. The Crystallinity Index (CrI) of (a) Birch and (b) Ash. Different lowercase letters above columns indicate a difference at a 0.05 level.

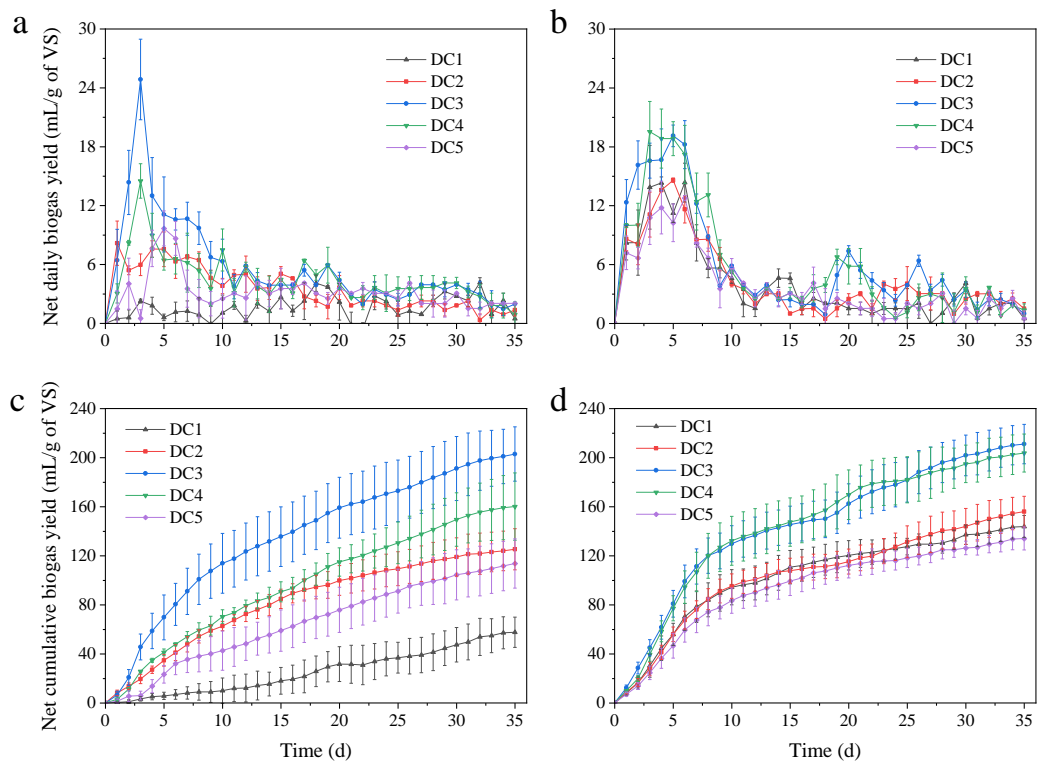


Fig. 4. Effect of different decay classes of wood samples on the biogas yield. Daily biogas yield of (a) Birch and (b) Ash, and net cumulative biogas yield of (c) Birch and (d) Ash.

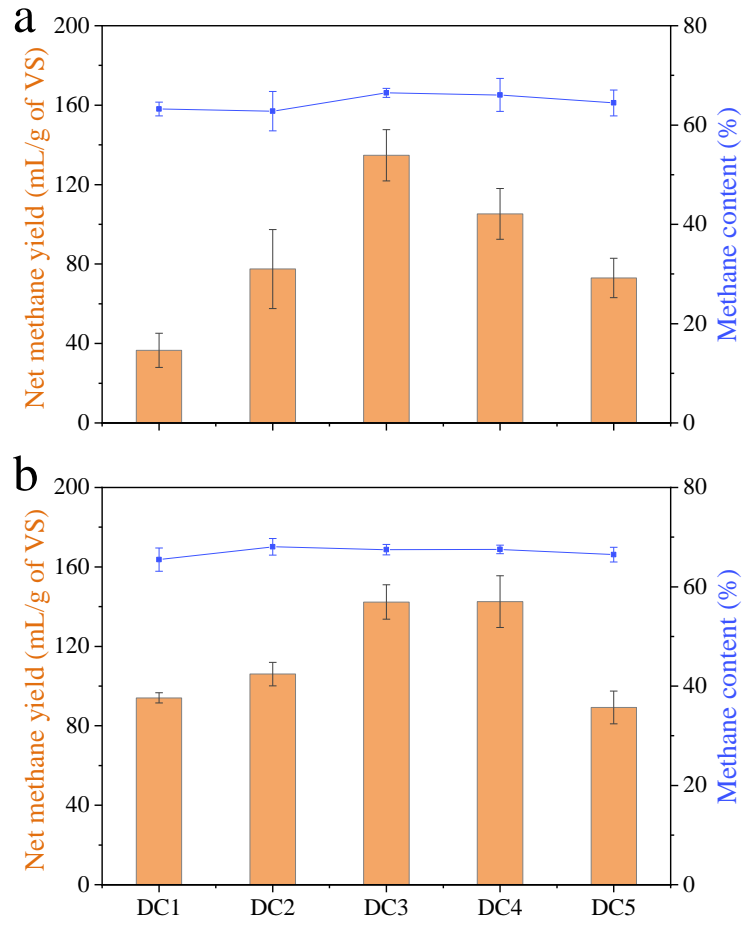


Fig. 5. The methane content and net methane yield of (a) Birch and (b) Ash wood samples for five decay classes.

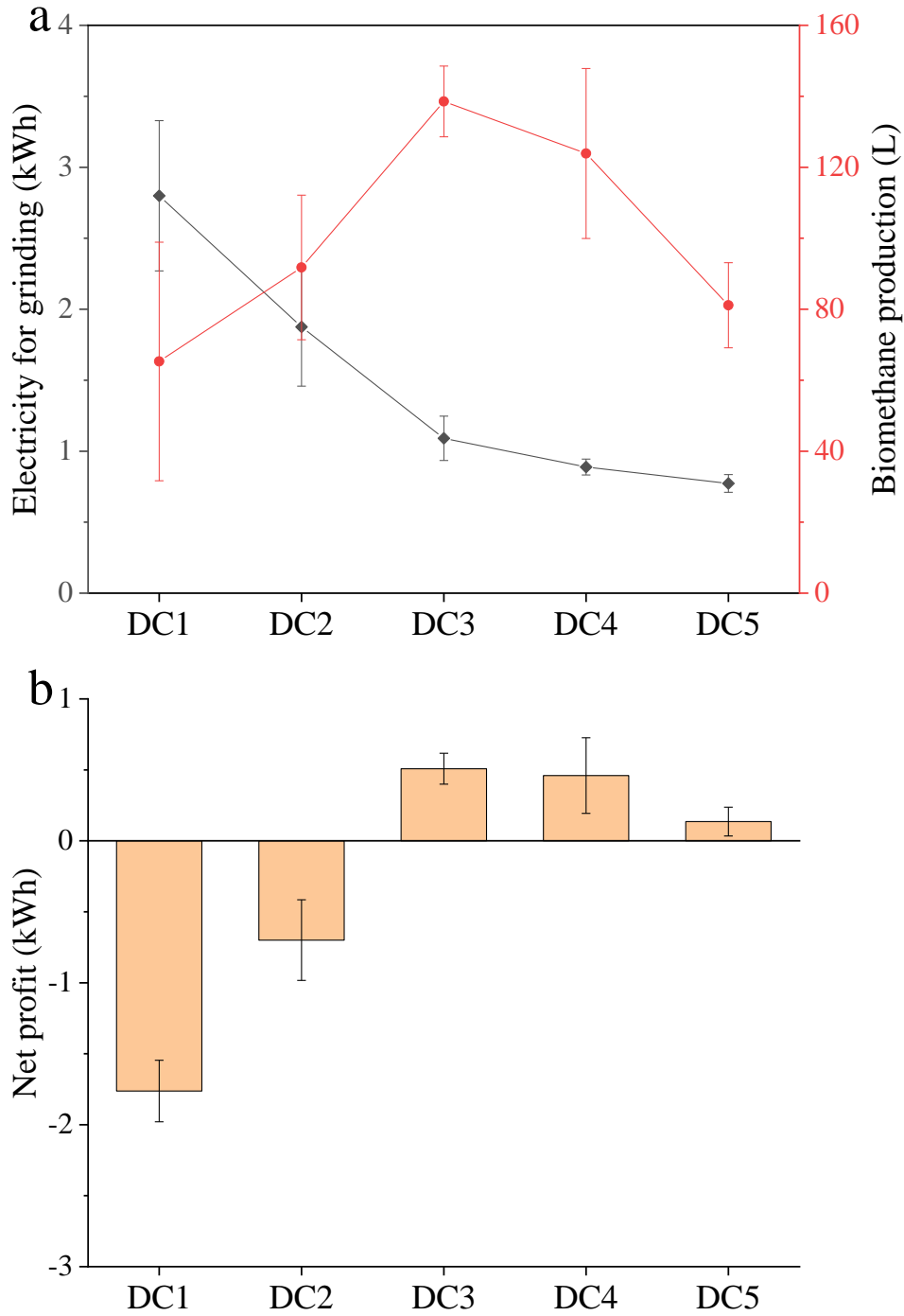


Fig. 6. The net profit analysis of anaerobic digestion for processing 1 kg of samples from five decay classes. (a) The average electricity consumption for grinding and methane production from wood samples; (b) The net energy output, calorific value of methane production minus electricity consumption.

Table 1. The particle size distribution, MWD, and FD of wood samples after grinding by the knife mill.

Wood type	Decay class	Proportion of wood mass in particle size class (%)							MWD (mm)	FD
		>2 mm	1–2 mm	0.5–1 mm	0.25–0.5 mm	0.125–0.25 mm	0.075–0.125 mm	<0.075mm		
Birch	DC1	2.12 ± 0.35	41.95 ± 5.60	30.31 ± 0.36	14.71 ± 2.91	6.82 ± 1.31	2.27 ± 0.59	1.83 ± 0.78	0.93 ± 0.07	1.85 ± 0.13
	DC2	0.31 ± 0.01	29.70 ± 0.89	26.80 ± 3.09	23.32 ± 3.81	9.59 ± 1.54	5.86 ± 0.66	4.42 ± 0.57	0.76 ± 0.00	2.15 ± 0.01
	DC3	0	21.27 ± 1.73	23.94 ± 3.02	19.32 ± 0.18	22.69 ± 1.92	7.92 ± 3.12	4.85 ± 3.73	0.62 ± 0.05	2.22 ± 0.19
	DC4	0	23.52 ± 0.64	27.72 ± 0.53	18.20 ± 2.83	15.89 ± 2.70	9.49 ± 1.27	5.18 ± 0.02	0.67 ± 0.02	2.26 ± 0.02
	DC5	0	16.75 ± 1.03	24.89 ± 4.54	23.66 ± 6.02	17.78 ± 1.57	9.92 ± 0.04	7.01 ± 1.08	0.57 ± 0.03	2.34 ± 0.03
Ash	DC1	1.51 ± 0.14	56.41 ± 2.55	28.49 ± 1.82	8.03 ± 0.53	3.48 ± 0.26	1.32 ± 0.10	0.76 ± 0.11	1.10 ± 0.03	1.57 ± 0.03
	DC2	0.75 ± 0.12	52.80 ± 0.45	29.39 ± 0.01	9.78 ± 0.28	4.12 ± 0.22	1.72 ± 0.02	1.45 ± 0.10	1.06 ± 0.01	1.74 ± 0.02
	DC3	0.14 ± 0.04	36.21 ± 0.97	29.62 ± 2.07	19.81 ± 1.02	9.78 ± 0.33	2.64 ± 0.02	1.80 ± 0.18	0.86 ± 0.00	1.90 ± 0.02
	DC4	0	32.78 ± 6.26	37.83 ± 0.58	17.31 ± 3.93	7.16 ± 1.21	3.09 ± 0.24	1.84 ± 0.78	0.86 ± 0.10	1.88 ± 0.14
	DC5	0	29.68 ± 2.63	31.63 ± 1.96	19.88 ± 0.38	10.69 ± 2.56	5.27 ± 0.21	2.86 ± 0.48	0.78 ± 0.04	2.06 ± 0.02

MWD: mean weight diameter (mm), FD: fractal dimension.

Table 2. Properties of decaying wood samples and inoculum in this study.

Properties	Birch					Ash					Inoculum
	DC1	DC2	DC3	DC4	DC5	DC1	DC2	DC3	DC4	DC5	
pH value	ND	ND	ND	ND	ND	ND	ND	ND	ND	ND	8.41 ± 0.36
Total solid (%)	59.47 ± 15.12	34.90 ± 3.81	26.30 ± 6.44	22.36 ± 10.16	18.39 ± 6.80	90.73 ± 1.79	87.81 ± 0.03	81.39 ± 5.70	80.84 ± 9.06	77.19 ± 6.35	8.14 ± 0.05
Volatile solid (%)	99.31 ± 0.60	99.08 ± 0.61	96.95 ± 0.40	97.28 ± 1.52	96.61 ± 0.73	98.05 ± 0.80	98.77 ± 0.11	98.31 ± 0.79	95.74 ± 2.96	97.25 ± 0.08	69.09 ± 0.11
<i>Ultimate analysis</i>											
Carbon (%)	47.16 ± 0.29	48.46 ± 0.87	47.56 ± 1.00	47.62 ± 1.45	50.55 ± 0.77	47.60 ± 0.40	47.19 ± 0.12	47.96 ± 0.04	48.41 ± 0.38	47.59 ± 0.40	31.80 ± 0.83
Nitrogen (%)	0.33 ± 0.04	0.84 ± 0.18	0.77 ± 0.19	1.18 ± 0.24	1.19 ± 0.10	0.13 ± 0.00	0.20 ± 0.10	1.40 ± 0.28	1.90 ± 0.08	1.77 ± 0.35	5.40 ± 0.08
Hydrogen (%)	5.76 ± 0.15	5.52 ± 0.16	5.53 ± 0.20	5.54 ± 0.22	5.45 ± 0.16	5.47 ± 0.14	5.62 ± 0.07	5.67 ± 0.06	5.77 ± 0.05	5.73 ± 0.01	5.07 ± 0.25
Oxygen (%)	44.76 ± 0.71	43.49 ± 1.06	44.04 ± 0.77	43.96 ± 1.27	41.26 ± 0.18	46.82 ± 0.52	46.98 ± 0.14	44.97 ± 0.19	43.92 ± 0.41	44.92 ± 0.63	36.20 ± 0.08
C/N ratio	146.73 ± 17.62	60.43 ± 12.92	65.82 ± 16.24	42.47 ± 10.46	42.92 ± 3.93	465.76 ± 104.05	302.11 ± 146.92	35.80 ± 7.32	25.49 ± 0.86	27.84 ± 4.91	5.89 ± 0.07
<i>Biochemical analysis</i>											
Extraction (%)	7.18 ± 0.59	5.06 ± 0.59	4.24 ± 0.75	3.94 ± 0.13	3.67 ± 1.31	8.47 ± 0.97	8.14 ± 0.45	6.77 ± 0.12	6.78 ± 0.65	3.90 ± 0.19	ND
Hemicelluloses (%)	23.37 ± 0.61	19.07 ± 1.04	22.41 ± 2.28	22.37 ± 0.60	17.94 ± 0.42	22.46 ± 2.19	22.01 ± 0.48	20.44 ± 0.05	22.45 ± 1.19	27.25 ± 0.72	ND
Cellulose (%)	34.29 ± 2.38	28.51 ± 1.09	27.09 ± 1.02	24.83 ± 1.50	16.24 ± 1.33	38.64 ± 1.17	34.15 ± 0.75	31.03 ± 1.38	28.35 ± 0.77	19.26 ± 0.72	ND
Lignin (%)	23.67 ± 2.07	34.85 ± 2.30	35.78 ± 2.70	35.63 ± 0.48	49.17 ± 1.90	26.88 ± 0.47	31.19 ± 1.04	38.33 ± 1.19	38.86 ± 0.35	44.61 ± 1.26	ND

ND: not determined. The % content of total solid was calculated based on wet mass; others were based on dry mas

